INFORMATION TO USERS

This was produced from a copy of a document sent to us for microfilming. While the most advanced technological means to photograph and reproduce this document have been used, the quality is heavily dependent upon the quality of the material submitted.

The following explanation of techniques is provided to help you understand markings or notations which may appear on this reproduction.

1. The sign or "target" for pages apparently lacking from the document photographed is "Missing Page(s)". If it was possible to obtain the missing page(s) or section, they are spliced into the film along with adjacent pages. This may have necessitated cutting through an image and duplicating adjacent pages to assure you of complete continuity.

2. When an image on the film is obliterated with a round black mark it is an indication that the film inspector noticed either blurred copy because of movement during exposure, or duplicate copy. Unless we meant to delete copyrighted materials that should not have been filmed, you will find a good image of the page in the adjacent frame.

3. When a map, drawing or chart, etc., is part of the material being photographed the photographer has followed a definite method in "sectioning" the material. It is customary to begin filming at the upper left hand corner of a large sheet and to continue from left to right in equal sections with small overlaps. If necessary, sectioning is continued again—beginning below the first row and continuing on until complete.

4. For any illustrations that cannot be reproduced satisfactorily by xerography, photographic prints can be purchased at additional cost and tipped into your xerographic copy. Requests can be made to our Dissertations Customer Services Department.

5. Some pages in any document may have indistinct print. In all cases we have filmed the best available copy.

University
Microfilms
International

300 N. ZEEB ROAD, ANN ARBOR, MI 48106
18 BEDFORD ROW, LONDON WC1R 4EJ, ENGLAND

Downloaded from SHAREOK. Persistent Handle URL: https://hdl.handle.net/11244/4698

8016924

CHENG, MO CHUN

TWO-DIMENSIONAL SIMULATION OF HEAT AND FLUID FLOW IN GEOTHERMAL SYSTEMS

The University of Oklahoma PH.D. 1980

University Microfilms International 300 N. Zeeb Road, Ann Arbor, MI 48106 18 Bedford Row, London WC1R 4EJ, England

Copyright 1980

by

CHENG, MO CHUN

All Rights Reserved

THE UNIVERSITY OF OKLAHOMA

GRADUATE COLLEGE

TWO-DIMENSIONAL SIMULATION OF HEAT AND FLUID FLOW IN GEOTHERMAL SYSTEMS

A DISSERTATION

SUBMITTED TO THE GRADUATE FACULTY

in partial fulfillment of the requirements for the

degree of

DOCTOR OF PHILOSOPHY

BY

MO CHUN CHENG

Norman, OKLAHOMA

1980

TWO-DIMENSIONAL SIMULATION OF HEAT AND FLUID FLOW IN

GEOTHERMAL SYSTEMS

A DISSERTATION

APPROVED FOR THE SCHOOL OF PETROLEUM AND GEOLOGICAL ENGINEERING

BY

This dissertation is dedicated to my parents

Mr. and Mrs. Kay-Yu Cheng

and my wife

Rebecca Chun-Ying Cheng

Acknowledgments

The author wishes to express his sincere appreciation to his dissertation committee members, Dr. H.B. Crichlow, Dr. A.W. McCray, Dr. D.E. Menzie, all of School of Petroleum and Geological Engineering, Dr. J.E. Fagan, School of Electrical Engineering and Computing Sciences, and Dr. F.M. Townsend, School of Chemical Engineering and Materials Sciences.

The author is particularly indebted to his dissertation adviser, Dr. H.B. Crichlow, who gave so generously of his precious time throughout the investigation and preparation of this dissertation. His guidance, support, patience, encouragement, understanding, inspiration, humor and philosophy made this dissertation possible.

The author is also indebted to his parents who have supported his education and who are responsible in the first place for teaching him the importance and necessity of education.

Finally, I am indebted to my wife, Rebecca Chun-Ying Cheng, who not only gave continous encouragement and support for my dissertation but also suffered from spending countless number of hours and hours and hours without me.

List of Figures

1	Pressure-enthalpy diagram	15
2	Development of model equations	16
3	Block-centered grid	20
4	Cell configuration	21
5	Flowchart: main algorithm	37
6	Interblock cell configuration	72
7	Reservoir grid for Mercer and Faust problem	77
8	Reservoir grid for East Mesa field problem	87

List of Tables

1	Data given in Mercer and Faust	78
2	Program run parameters	79
3	Simulation results of Mercer and Faust problem $\Delta t = 0.259200 \times 10^7$ sec (30 days)	80
4	Comparisions between CGS results and those of Mercer and Faust	82
5	Number of iterations per time step	83
6	Simulation results of Mercer and Faust problem $\Delta t = 1.555200 \times 10^7$ sec (180 days)	85
7	Data for East Mesa field problem	88
8	Simulation results of East Mesa field problem	89

List of Simulator (CGS) Routines

CGS MAIN	48
ALSIP	51
CELL	51
COEH	52
COEP	53
CONTER	53
FUNPHA	54
GRID	60
HSHW	60
INPUT	61
MBC2	62
METDER	63
OUTCEL	64
OUTIN	65
POR	66
PREDIH	66
RELAX	67
RELPER	67
RESULT	68
ROCKH	69
SIP	70
TITLE	71
TRANSM	71

UPSTRM 72

WELL 73

CONTENTS

	Acknowledgment	iv
	List of Figures	v
	List of Tables	vi
	List of Simulator (CGS) Routines	vii
	CHAPTER ONE	
	INTRODUCTION	
1.1	Introduction to Geothermal Reservoirs	1
1.2	Geothermal Reservoir Simulation	1
1.3	Statement of the Problem	3
1.4	Literature Review	5
	CHAPTER TWO	
	MODELING AND SIMULATION	
2.1	Model	13
2.2	Development of Model Equations	14
2.3	Finite Difference Analog	20
2.4	Solution Method	29
2.5	Matrix Solution Method: SIP	38

2.6 Computer Geothermal Simulator: CGS 47

2.7 Simulator Subroutines 51

CHAPTER THREE

RESULTS

3.1 Testing of Simulator: CGS 76

3.2 Simulation Results 1: Mercer and Faust Problem 76

3.3 Simulation Results 2: East Mesa Field Problem 85

3.4 Conclusions 90

Nomenclature 92

References 96

Appendix 100

A Sample of CGS Output

CHAPTER ONE

INTRODUCTION

1.1 Introduction to Geothermal Reservoirs

Geothermal reservoirs can be classified into three types as compressed-water type (one-phase), water-steam type (two-phase) and superheated-steam type (one-phase). In compressed-water type, the pressure controlling phase is the one-phase liquid water. Examples are the Wairekei field in New Zealand and the Cerro Prieto field in Mexico. In water-steam type, either liquid water and/or steam can be the pressure controlling phase(s), depending on the saturation of each phase. This type of reservoir usually results from the producing of geothermal fluid of the other two types. In superheated-steam type, the pressure controlling phase is the one-phase vapor steam. Examples are the Geysers in California and the Lardarello field in Italy. Among the three, the first is probably the most common in the world. Today, the generation of electricity from geothermal reservoir fluid is the main application of the geothermal resources.

1.2 Geothermal Reservoir Simulation

The knowledge of petroleum reservoir simulation has been used

for studying the behavior of geothermal reservoirs (1,2). Thus, a compressed-water type can be considered as a single-phase oil reservoir, a superheated-steam type as a dry gas reservoir, etc. The objectives of geothermal simulation can be summarized by the following:

1. To estimate fluid and energy reserves.
2. To obtain information about the geothermal system --- boundary conditions, reservoir geometry, rock properties, etc.
3. To study subsidence effects as a result of the unusually large withdrawal of fluid (in terms of millions of pounds of water per day) from the geothermal system.
4. To study thermodynamic changes on the produced and the reinjected geothermal fluids.
5. To study the effects of reinjection of produced geothermal fluid into the system.
6. To study the environmental effects of the dissolved gases (like NH_3 , H_2S) in geothermal fluid.

The injection of produced geothermal fluid back into the geothermal system is especially important. This process serves three main purposes. First, probably the most important, it helps maintain the pressure and heat in the reservoir. Second, it can minimize the subsidence of the reservoir (if any) as discussed before. Third, it can solve the problem of 'waste' geothermal fluid disposal.

The economics of the operation of a geothermal power plant lies in the fact that the maximum amount of heat be extracted for the producing life span of the geothermal reservoir. For a given size of reservoir and a given rated power plant, it is desirable to keep

the system operating for a given life span, e.g. 25 years. The reason is obvious. The investment in a geothermal power plant is a multi-million project that requires the returning revenues be paid off in its future operating period. A power plant built to operate for just a few years will be a disastrous investment.

The objective of operating a geothermal power plant for a certain desired period of time can be done by careful management of the geothermal reservoir. Thus, injection and production rates are to be selected such that the reservoir is not producing too slow to give insufficient amount of heat to drive the power plant and the reservoir is not depleting too fast to shorten its producing life span. In addition, spacing of injection and production wells is significant. Injection fluid rates and temperatures must be chosen such that the reservoir pressure is kept to a certain limit and at the same time early breakthrough of the injection fluid cool fronts at the different production wells are to be avoided. A cool front is usually at a relatively lower temperature than that of the geothermal fluid in a production well. Actually, when a cool front arrives at a production well, the operating economics of the well is over, for it no longer can deliver enough heat to the power plant. Through judicious reservoir simulation work and economic analysis, the optimization of the maximum recovery of heat in a desirable period of time may be achieved.

1.3 Statement of the Problem

The development and the applications of an efficient two-dimensional (x-y), two-phase, finite difference type geothermal reservoir simulator

is the objective of this study. The simulator can be used to simulate a geothermal reservoir of any of the three types discussed earlier. Sinks and sources can be included in the simulator, allowing the study of the production and reinjection of geothermal fluids from and into the reservoir.

However, geothermal reservoir simulation is not without its difficulties. The simulation of the geothermal system involves the transport of both fluid and heat, opposed to that of fluid only in the usual black oil reservoir simulation. This is further complicated by the fact that the geothermal fluid is usually not pure water but rather water of high salinity and composed of different minerals like silicon, magnesium, etc. The model describing the transport of fluid and heat in saline systems will have to take into considerations the effects such as lowering of water vapor pressure, changes in capillary pressure, as a result of the presence of the salt concentrations, along with the fluid being at a relatively high temperature (usually 200°C and above). Thus, a very complicated phase equilibria might occur (3). Also, little is known about the dependence of rock properties like porosity, permeability, on these chemical changes and at these high temperatures. Moreover, as a result of the changes of pressure and temperature, the fluid in certain geothermal reservoir grid blocks will change from one state to another during simulation. This problem will usually lead to unstable simulation computations as well as large material and energy balance errors. Finally, today the limited supply of reliable geothermal data precludes the comprehensive testing of the validity of geothermal simulators. As more data become available

in the future this testing will become routine.

1.4 Literature Review

The following presents a literature review on the mathematical simulation of geothermal reservoirs. The literature for geothermal reservoir simulation is relatively limited as compared to that of petroleum reservoir simulation. The reason is simply that the simulation of geothermal systems is still in its developmental stage.

Work of Whiting and Ramey (3)

Whiting and Ramey developed a zero-dimensional simulator including fluid influx by making use of the thermodynamic principles, material and energy balances. These authors indicated that the knowledge of mass withdrawals and the enthalpy of the fluid withdrawn was important for the modeling of geothermal reservoir. Their model can be used to estimate the initial conditions and to match the past performance history and predict the future performance of the geothermal reservoir. Using this model, the production data of the Wairakei geothermal field in New Zealand were matched successfully. The material-energy balance equation derived by these authors is:

$$W_p (h_p - E_c) + W_L (h_L - E_c) + Q = W \{ E_i - E_c + (\frac{1 - \phi}{\phi}) .$$

$$[x_i v_{gi} + (1 - x_i) v_{fi}] \rho_r C_{vr} (T_i - T_c) \} + (h_e - E_c) .$$

$$\frac{B}{v_{fe}} \Sigma Q_D (t_D) \Delta P_n$$

Work of Harlow and Pracht (4)

Harlow and Pracht performed a theoretical study of the extraction of geothermal energy from a dry geothermal well. Their model were combined equations describing the coupled process of rock fracture, fluid flow and heat transport of a single phase (compressed-water). From their example studies, they concluded that large amount of energy can be extracted from dry wells penetrating hot rock under favorable conditions. However, the authors did indicate that actual field data was significant for confirming their results.

Work of Gould (5)

Gould presented a geothermal wellbore model which included two-phase pressure drop, flow regime change, phase change, relative steam-water velocity and heat transfer from the fluid. This model can be used to calculate pressure, temperature and steam quality profiles in a geothermal wellbore. Their profiles can aid in the calculation of wellbore deliverability. Gould applied his model to study the Wairakei and the Broadlands geothermal fields of New Zealand. Over all, the model results matched fairly well with the field data.

Work of Faust and Mercer (2)

Faust and Mercer developed a Galerkin-finite element model for simulating vapor-dominated, two-phase, and liquid-dominated geothermal reservoir systems. The model is made up of two nonlinear partial differential equations derived from the conservation equations of mass, energy and momentum in porous media. Pressure and enthalpy are the dependent variables to be solved in the model. The authors applied

this model to study several hypothetical examples: one-dimensional, steady-state vertical flow, multiphase horizontal flow and two-dimensional horizontal flow. Their computed results agreed with the expected behavior of geothermal reservoirs.

Work of Garg et al. (6)

Garg et al. presented a finite difference model for simulating single- and two-phase geothermal fluid flow in one, two, or three dimensions. In this model, mixture (liquid-vapor) density, mixture energy, rock energy and mass transfer rate (from liquid to vapor) are the unknowns to be solved. These authors used this model to study transport of mass and energy in linear bench-scale laboratory models conducted at Stanford University. The theoretical and experimental results were in good agreement. Garg et al. also studied production and injection into a hypothetical geothermal reservoir by using this model and concluded that maximum gross power output could be obtained with reinjection of fluid into the geothermal reservoir.

Work of Lasseter et al. (7)

Lasseter et al. studied geothermal reservoirs by using a computer program called SHAFT (Simultaneous Heat and Fluid Transport). This computer model can be used to simulate one- or two-phase reservoirs for transient or steady state in one, two or three dimensions. Density and internal energy are the two unknowns to be solved in this finite difference model for strict guarantee of conservation of mass. The authors tested SHAFT by applying the

program to two hypothetical geothermal systems, one liquid-dominated, the other, vapor-dominated. However, no attempt was made to model actual field performance.

Work of Robinson and Morse (8)

Robinson and Morse developed a one-dimensional finite-difference geothermal model which included the effects of gravity, capillary pressure, phase change, heat conduction and convection. The authors used this model to study the effect of production rate on the ultimate heat produced for three hypothetical geothermal systems which were reservoirs with a finite water content, a low rate of water influx, and a high rate of water influx. From their studies, they concluded that pressure in liquid-dominated reservoir should be reduced for in-situ flashing of water to steam for best production. Also, the reinjection of fluid into a liquid-dominated reservoir would not give significant improvement in heat extraction except in reservoir with low porosity.

Work of Mercer and Faust (9)

Mercer and Faust presented a geothermal model similar to that of Faust and Mercer (2). The model is capable of simulating transport of heat and flow of compressed-water, steam-water mixture, and superheated-steam in a porous medium. Fluid pressure and enthalpy are the two dependent variables. The authors applied this model and the Mercer's model (2) to study a hypothetical hot-water reservoir with initial conditions approximately equal to those in the Wairakei field in New Zealand. Results of both models agreed

very well. Also, a hypothetical vapor-dominated reservoir was simulated using this model and the Toronyi's model (1) . Again, the results of both models were very close.

Work of Tansev et al. (10)

Tansev et al. developed a wellbore model that combined equations for heat transfer, vertical pressure drop and pump capacity to simulate two-phase steady-state flow behavior of a geothermal well. Pressure, temperature and quality were solved as a function of depth. This model was used to study the data from the Broadlands and Wairakei field in New Zealand, the Otake field in Japan and the Imperial Valley in California. The calculated results (chiefly wellhead parameters) matched very well with all the field data except those from the Imperial Valley. The authors concluded that the model can be used to determine an optimal flow rate for a geothermal well, design well completions, predict available energy at the wellhead, etc.

Work of Toronyi and Farouq Ali (1,11)

Toronyi and Farouq Ali presented a simulator for studying production from a two-phase geothermal reservoir. The simulator is made up of a reservoir model and a wellbore model which are coupled together. The reservoir model is a finite-difference, two-dimensional, two-phase model that describes the flow of mass and heat of fluid within an anisotropic, heterogeneous porous medium. The wellbore model is a one-dimensional model that describes the flow of a homogeneous, two-phase mixture. Pressure, water saturation, and pressure, quality are the unknown variables to be solved in the reservoir model and the

wellbore model respectively. From the simulation study, the authors classified two-phase geothermal reservoir into three types: vapor-dominated, liquid-dominated, and mixed domination. Also, reservoirs of low porosity and permeability type were good candidates for forming superheated regions.

Work of Martin (12)

Martin analyzed internal steam drive in geothermal reservoir by applying the model for solution gas drive in petroleum reservoir. In this geothermal model, hot water and steam production are determined by their respective mobilities. By studying the plots of pressure vs cumulative fluid production, pressure vs cumulative heat produced, the authors concluded that hot-water reservoirs can have complicated production performance. Also, more extraction of heat can be done by setting wells high in the reservoir to increase steam production and decrease water production. More importantly, the authors indicated that petroleum reservoir engineering can be applied to geothermal systems that involve the flow of fluid in porous media.

Work of Faust and Mercer (13)

Faust and Mercer presented a two-dimensional, finite-difference model for simulating liquid- and vapor-dominated geothermal reservoirs. The model is based on the equations developed in the Galerkin-finite element simulator of Mercer and Faust (9); fluid pressure and enthalpy are the unknown dependent variables. The authors used this finite difference model to study several examples and campared the results obtained with those of the finite element model. Based on

their comparision, they concluded that the finite element model is adequate for single-phase reservoir, which permits better approximations of boundary and internal geometries while the finite difference model is more suitable for two-phase reservoir, which results in stable calculations. Also, coning and percolation were mentioned as difficult problems in geothermal reservoir simulation.

Work of Brigham and Morrow (14)

Brigham and Morrow analyzed geothermal reservoirs by studying the plots of p/Z (p=pressure, Z=compressibility) vs fraction of fluid produced. They studied three basic geothermal systems. The first is a steam type. The second is a water-steam one. And the third is a water type. From their studies, they concluded that low porosity would give correct plots. Also, it is desirable to locate boiling water existing deep in a reservoir. Furthermore, the authors indicated that pressure, temperature, and enthaply measurements of geothermal steam cannot be used as complete indicators for determining the original state of the geothermal system.

Work of Thomas and Pierson (15)

Thomas and Pierson developed a three-dimensional finite difference model for the simulation of geothermal reservoirs. The model is adequate for reservoirs that contain water in any of its vapor or liquid states. The unique feature of the model is that it includes treatment for changes of states during a time step, which results in very stable calculations and minimum pressure, heat balances and material balances errors. The model can be used to study entire

field, cross-sectional or individual well systems. The authors compared their model results with those of Toronyi's two-phase problem and those of Stanford two-phase problem. The results agreed. They also studied a three-dimensional example and a radial example. Based on their studies, the authors claimed that their simulator was a very comprehensive and stable one. Also, they indicated that the formation of superheated-steam is dependent upon the pressure decline in a geothermal reservoir.

CHAPTER TWO

MODELING AND SIMULATION

2.1 Model

The two-dimensional geothermal reservoir simulator developed in this study follows that of Mercer and Faust (9,13). The model describing the horizontal transport of fluid and heat in a geothermal reservoir can be represented by the following two simultaneous nonlinear partial differential equations:

$$\nabla \cdot \left(\frac{b\rho_s k k_{rs}}{\mu_s} \nabla P \right) + \nabla \cdot \left(\frac{b\rho_w k k_{rw}}{\mu_w} \nabla P \right) + bq_s + bq_w = b \frac{\partial (\phi \rho)}{\partial t} \qquad (1)$$

$$\nabla \cdot \left(\frac{b\rho_s h_s k k_{rs}}{\mu_s} \nabla P \right) + \nabla \cdot \left(\frac{b\rho_w h_w k k_{rw}}{\mu_w} \nabla P \right) + \nabla \cdot \{ K_m b [(\frac{\partial T}{\partial P})_h \nabla P + (\frac{\partial T}{\partial h})_P \nabla h] \} + bq_s h_s + bq_w h_w = b \frac{\partial}{\partial t} [\phi \rho h + (1 - \phi) \rho_r h_r] \qquad (2)$$

with Neumann boundary conditions:

at $x = 0$ and $x = L$,

$$\frac{\partial P}{\partial x} = 0 \qquad (3)$$

$$\frac{\partial h}{\partial x} = 0 \qquad (4)$$

at $y = 0$ and $y = W$,

$$\frac{\partial P}{\partial y} = 0 \qquad (5)$$

$$\frac{\partial h}{\partial y} = 0 \qquad (6)$$

where

P = geothermal fluid pressure = $P(x,y,t)$

h = geothermal fluid enthalpy = $h(x,y,t)$

$$\nabla \cdot = \frac{\partial}{\partial x} + \frac{\partial}{\partial y}$$

$$\nabla = i\frac{\partial}{\partial x} + j\frac{\partial}{\partial y}$$

for other notations, see nomenclature.

2.2 Development of Model Equations

The geothermal fluid in this study is assumed to be pure water and as such the state of the fluid can be determined by the use of the pressure-enthalpy diagram for pure water (fig.1) if pressure and enthalpy of the geothermal fluid are known.

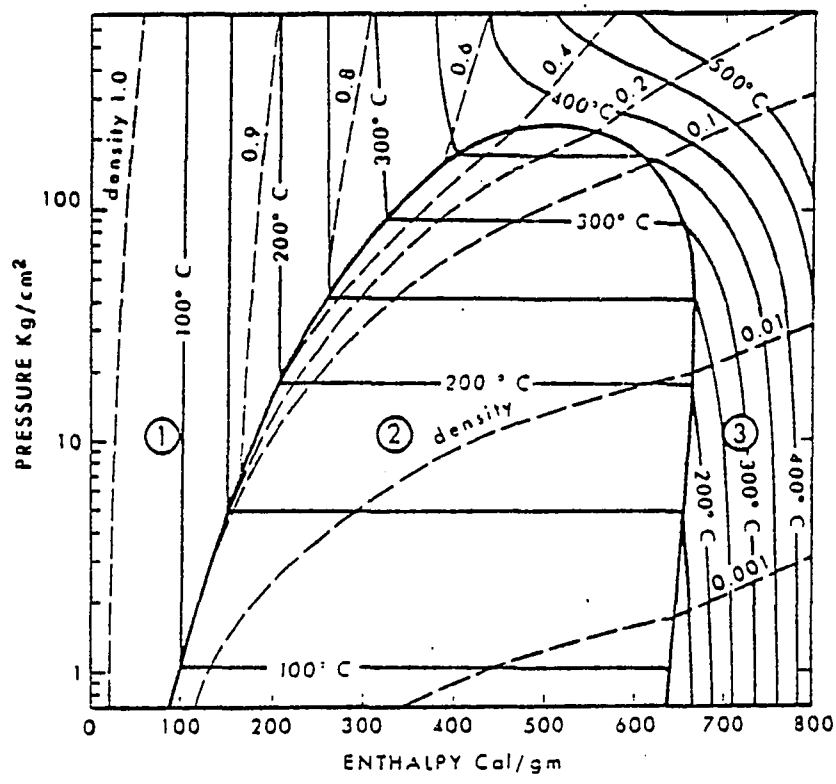

Fig. 1 Pressure-enthalpy diagram (equation of state) for pure water and vapor showing three thermodynamic regions below the critical point (apex of parabola): (1) compressed-water, (2) two-phase steam-water, and (3) superheated-steam (after White, et al. (16))

Eqs. (1) and (2) use pressure P and enthalpy h as the unknown dependent variables. The solution of these two equations will give the pressure and enthalpy distributions of the geothermal reservoir under concern. Once these two are obtained, the other PVT properties of the geothermal fluid such as temperature, water saturation, etc. expressed as functions of P and h, can be computed. The basic approach to derive eqs. (1) and (2) can be summarized by the following diagram:

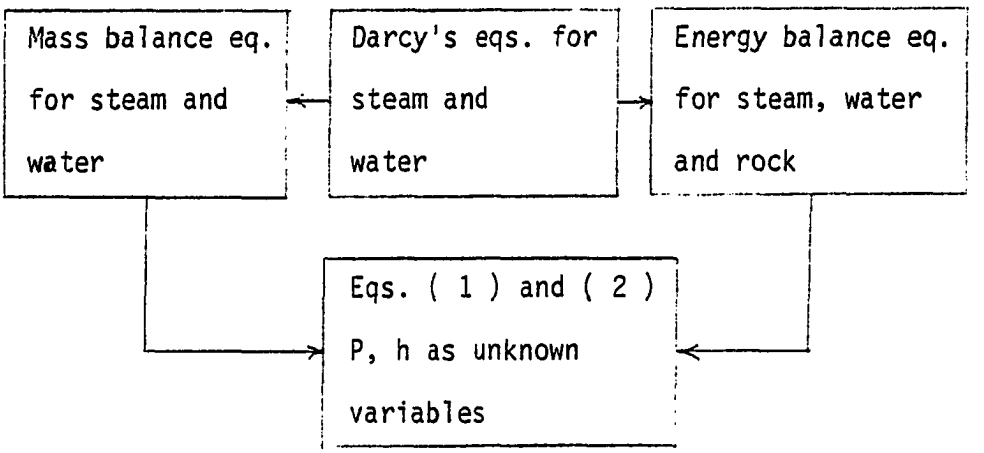

Fig. 2 Development of model equations

Consider a differential volumetric element of a geothermal reservoir. This element is consisted of compound water (liquid water and/or vapor steam) and rock (solid).

The mass balance eq. with a point sink term (9) is

$$b \frac{\partial}{\partial t} \left[\phi S_s \rho_s + \phi S_w \rho_w \right] + b \nabla . (\rho_s \bar{v}_s) + b \nabla . (\rho_w \bar{v}_w) - b q_s - b q_w = 0 \qquad (7)$$

with

$$\phi = \phi (P) \qquad (8)$$

$$\rho_s = \rho_s (P,h) \qquad (9)$$

$$\rho_w = \rho_w (P,h) \qquad (10)$$

and $$S_s + S_w = 1 \qquad (11)$$

Define $\rho = S_s\rho_s + S_w\rho_w$, (12)

eq. (7) becomes

$$b\frac{\partial(\phi\rho)}{\partial t} + b\nabla\cdot(\rho_s\bar{v}_s) + b\nabla\cdot(\rho_w\bar{v}_w)$$

$$- bq_s - bq_w = 0 \qquad (13)$$

The energy balance equation in terms of enthalpies with a point heat sink term (9) is

$$b\frac{\partial}{\partial t}\left[\phi(S_s\rho_s h_s + S_w\rho_w h_w) + (1-\phi)\rho_r h_r\right]$$

$$+ b\nabla\cdot(\rho_s h_s\bar{v}_s + \rho_w h_w\bar{v}_w) + b\nabla\cdot(\bar{\lambda}_s + \bar{\lambda}_w + \bar{\lambda}_r)$$

$$- bq_s h_s - bq_w h_w = 0 \qquad (14)$$

where

$$h_s = U_s + \frac{P}{\rho_s} \qquad (15)$$

$$h_w = U_w + \frac{P}{\rho_w} \qquad (16)$$

$$h_r = U_r + \frac{P}{\rho_r} \qquad (17)$$

Eq. (14) assumes capillary pressure P_c to be negligible:

$$P_c = P_s - P_w = 0 \qquad (18)$$

$$\text{or} \quad P_s = P_w = P \qquad (19)$$

Also, compressible work is neglected in eq. (14).

$$\text{Define} \quad h = \frac{S_s \rho_s h_s + S_w \rho_w h_w}{\rho} \qquad (20)$$

$$\text{and} \qquad \bar{\lambda}_m = \bar{\lambda}_s + \bar{\lambda}_w + \bar{\lambda}_s \qquad (21)$$

$\bar{\lambda}_m$ represents the medium conduction/dispersion flow term (9) which is given by

$$\bar{\lambda}_m = - K_m . \nabla T \qquad (22)$$

with

$$K_m = K_m (x,y) \qquad (23)$$

Eq. (14) can now be written as

$$b \frac{\partial}{\partial t} \left[\phi \rho \left(\frac{S_s \rho_s h_s + S_w \rho_w h_w}{\rho} \right) + (1 - \phi) \rho_r h_r \right]$$

$$+ b \nabla . (\rho_s h_s \bar{v}_s + \rho_w h_w \bar{v}_w) + b \nabla . \bar{\lambda}_m$$

$$- b q_s h_s - b q_w h_w = 0 \qquad (24)$$

or

$$b\frac{\partial}{\partial t}\left[\phi\rho h + (1 - \phi) \rho_r h_r\right] + b \nabla . (\rho_s h_s \bar{v}_s + \rho_w h_w \bar{v}_w)$$

$$- b \nabla . (K_m \nabla T) - bq_s h_s - bq_w h_w = 0 \qquad (25)$$

Darcy's equations for steam and water neglecting gravity segregation are

$$\bar{v}_s = - \frac{kk_{rs}}{\mu_s} \nabla P \quad , \qquad (26)$$

$$\bar{v}_w = - \frac{kk_{rw}}{\mu_w} \nabla P \qquad (27)$$

with

$$k = k (x,y) \qquad (28)$$

$$k_{rs} = k_{rs} (S_w, S_s) \qquad (29)$$

$$k_{rw} = k_{rw} (S_w, S_s) \qquad (30)$$

$$\mu_s = \mu_s (T) \qquad (31)$$

$$\mu_w = \mu_w (T) \qquad (32)$$

Put eqs. (26) and (27) in eq. (13):

$$\nabla . \left(\frac{b\rho_s kk_{rs}}{\mu_s} \nabla P \right) + \nabla . \left(\frac{b\rho_w kk_{rw}}{\mu_w} \nabla P \right)$$

$$+ bq_s + bq_w = b \frac{\partial (\phi\rho)}{\partial t} \qquad (1)$$

With $T = T (P,h)$, (33)

$$\nabla T = (\frac{\partial T}{\partial P})_h \nabla P + (\frac{\partial T}{\partial h})_p \nabla h \qquad (34)$$

and eqs. (26) and (27), eq. (25) becomes

$$\nabla . (\frac{b \rho_s h_s kk_{rs}}{\mu_s} \nabla P) + \nabla . (\frac{b\rho_w h_w kk_{rw}}{\mu_w} \nabla P)$$

$$+ \nabla . \{ K_m b [(\frac{\partial T}{\partial P})_h \nabla P + (\frac{\partial T}{\partial h})_p \nabla h] \}$$

$$+ bq_s h_s + bq_w h_w = b \frac{\partial}{\partial t} [\phi\rho h + (1 - \phi) \rho_r h_r] \qquad (2)$$

2.3 Finite Difference Analog

The block-centered type grid (17) is used for formulating the finite difference equations for eqs. (1) and (2):

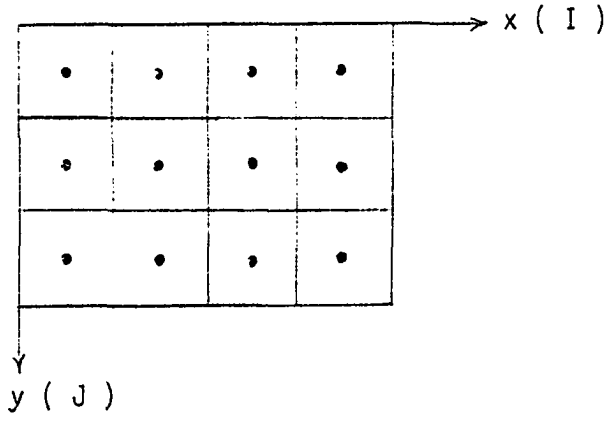

Fig. 3 Block-centered grid

Each finite difference equation is to be written on each cell of the grid:

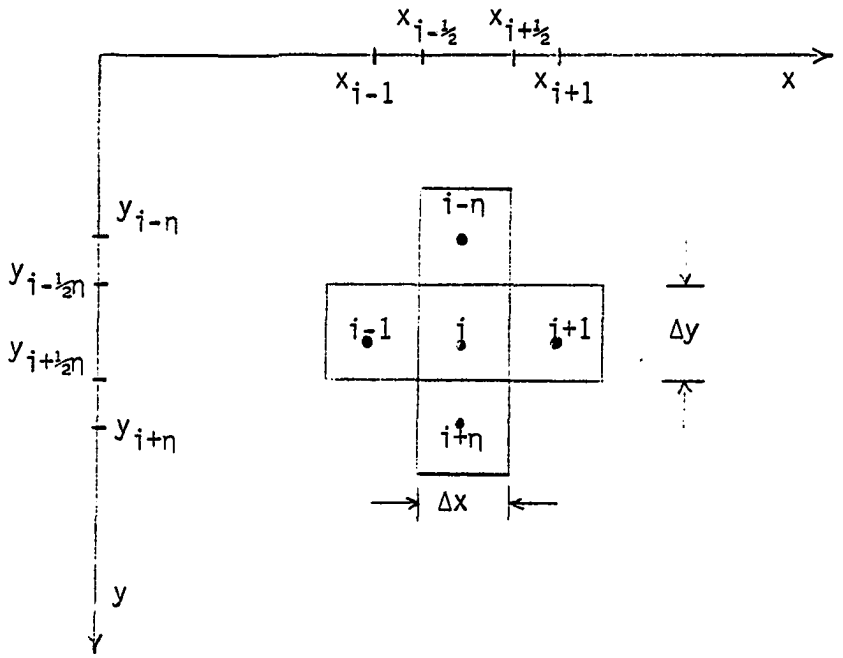

i : cell index

η : maximum number of cells in the x-direction

Fig. 4 Cell configuration

In this study, single indexing is utilized to identify functions written within the two-dimensional (x-y) region. Thus,

$$p_i^n = P\ (\ x_i, y_i, n\ ) \qquad (\ 35\ )$$

$$h_i^n = h\ (\ x_i, y_i, n\ ),\ \text{etc.} \qquad (\ 36\ )$$

where n is the time level.

The use of single indexing for identifying the difference variables is for the ease of coding these variables in single dimensioning in the computer simulator program developed later. The advantage of doing this is that the use of single dimensioning is more efficient for the computer to handle than that of double dimensioning, which must be used as a result of using double indexing of the unknown variables.

Consider eqs. (1) and (2).

Multiply eq. (1) by V/b :

$$\nabla \cdot \left(kV \frac{\rho_s k_{rs}}{\mu_s} \nabla P \right) + \nabla \cdot \left(kV \frac{\rho_w k_{rw}}{\mu_w} \nabla P \right) + V (q_s + q_w) = \frac{\partial (V \phi \rho)}{\partial t} \qquad (37)$$

With n as the old time level and n+1 as the current time level, the implicit finite difference analog for eq. (37) can be written as:

$$\left[\frac{k A_x}{\Delta x} \frac{\rho_s k_{rs}}{\mu_s} \right]_{i+\frac{1}{2}} (P_{i+1}^{n+1} - P_i^{n+1}) - \left[\frac{kA_x}{\Delta x} \frac{\rho_s k_{rs}}{\mu_s} \right]_{i-\frac{1}{2}} (P_i^{n+1} - P_{i-1}^{n+1})$$

$$+ \left[\frac{kA_x}{\Delta x} \frac{\rho_w k_{rw}}{\mu_w} \right]_{i+\frac{1}{2}} (P_{i+1}^{n+1} - P_i^{n+1}) - \left[\frac{kA_x}{\Delta x} \frac{\rho_w k_{rw}}{\mu_w} \right]_{i-\frac{1}{2}} (P_i^{n+1} - P_{i-1}^{n+1})$$

$$+ \left[\frac{kA_y}{\Delta y} \frac{\rho_s k_{rs}}{\mu_s} \right]_{i+\frac{1}{2}\eta} (P_{i+\eta}^{n+1} - P_i^{n+1}) - \left[\frac{kA_y}{\Delta y} \frac{\rho_s k_{rs}}{\mu_s} \right]_{i-\frac{1}{2}\eta} (P_i^{n+1} - P_{i-\eta}^{n+1})$$

$$+\left[\frac{kA_y}{\Delta y}\frac{\rho_w k_{rw}}{\mu_w}\right]_{i+\frac{1}{2}\eta}\left(p_{i+\eta}^{n+1}-p_i^{n+1}\right)-\left[\frac{kA_y}{\Delta y}\frac{\rho_w k_{rw}}{\mu_w}\right]_{i-\frac{1}{2}\eta}\left(p_i^{n+1}-p_{i-\eta}^{n+1}\right)$$

$$+Vq_t=\frac{\left(V\phi\rho\right)_i^{n+1}-\left(V\phi\rho\right)_i^n}{\Delta t} \qquad (38)$$

where

$$q_t = q_s + q_w \qquad (39)$$

$$\Delta t = t^{n+1} - t^n \qquad (40)$$

Δx, Δy = increment of x, y (41)

$$A_x = \frac{V}{\Delta x} \qquad (42)$$

$$A_y = \frac{V}{\Delta y} \qquad (43)$$

Let $M = V\phi\rho$ (44)

and define the following interblock transmissibility terms:

$$T_{sx} = \left(\frac{kA_x}{\Delta x}\right)\frac{\rho_s k_{rs}}{\mu_s} \qquad (45)$$

$$T_{sy} = \left(\frac{kA_y}{\Delta y}\right)\frac{\rho_s k_{rs}}{\mu_s} \qquad (46)$$

$$T_{wx} = \left(\frac{kA_x}{\Delta x}\right)\frac{\rho_w k_{rw}}{\mu_w} \qquad (47)$$

$$T_{wy} = \left(\frac{kA_y}{\Delta y} \right) \frac{\rho_w k_{rw}}{\mu_w} \qquad (48)$$

Using these, eq. (38) can be written as:

$$\Delta_x \left[\left(T_{wx} + T_{sx} \right) \Delta_x p^{n+1} \right] + \Delta_y \left[\left(T_{wy} + T_{sy} \right) \Delta_y p^{n+1} \right]$$

$$+ Vq_t = \frac{M^{n+1} - M^n}{\Delta t} \qquad (49)$$

where

$$\Delta_x \left(T_{wx} \Delta_x p^{n+1} \right) = T_{wx_{i+\frac{1}{2}}} \left(p_{i+1}^{n+1} - p_i^{n+1} \right) - T_{wx_{i-\frac{1}{2}}} \left(p_i^{n+1} - p_{i-1}^{n+1} \right) \qquad (50)$$

$$\Delta_y \left(T_{wy} \Delta_y p^{n+1} \right) = T_{wy_{i+\frac{1}{2}\eta}} \left(p_{i+\eta}^{n+1} - p_i^{n+1} \right) - T_{wy_{i-\frac{1}{2}\eta}} \left(p_i^{n+1} - p_{i-\eta}^{n+1} \right) \qquad (51)$$

Similar difference operations hold for T_{sx} and T_{sy} .

Eq. (49) is the implicit finite difference analog of eq. (1) in terms of finite difference operators and interblock transmissibility terms. A similar one developed for eq. (2) is as follows.

Multiply eq. (2) by V/b:

$$\nabla . \left(kV \frac{\rho_s k_{rs}}{\mu_s} h_s \nabla P \right) + \nabla . \left(kV \frac{\rho_s k_{rw}}{\mu_w} h_w \nabla P \right)$$

$$+ V \nabla . \left\{ K_m \left[\left(\frac{\partial T}{\partial P} \right)_h \nabla P + \left(\frac{\partial T}{\partial h} \right)_p \nabla h \right] \right\}$$

$$+ Vq_s h_s + Vq_w h_w = V \frac{\partial}{\partial t} \left[\phi \rho h + (1 - \phi) \rho_r h_r \right] \qquad (52)$$

The implicit finite difference analog for eq. (52) can be written as:

$$\left[\frac{kA_x}{\Delta x}\frac{\rho_s k_{rs}}{\mu_s}h_s\right]_{i+\frac{1}{2}}\left(P_{i+1}^{n+1}-P_i^{n+1}\right)-\left[\frac{kA_x}{\Delta x}\frac{\rho_s k_{rs}}{\mu_s}h_s\right]_{i-\frac{1}{2}}\left(P_i^{n+1}-P_{i-1}^{n+1}\right)$$

$$+\left[\frac{kA_x}{\Delta x}\frac{\rho_w k_{rw}}{\mu_w}h_w\right]_{i+\frac{1}{2}}\left(P_{i+1}^{n+1}-P_i^{n+1}\right)-\left[\frac{kA_x}{\Delta x}\frac{\rho_w k_{rw}}{\mu_w}h_w\right]_{i-\frac{1}{2}}\left(P_i^{n+1}-P_{i-1}^{n+1}\right)$$

$$+\left[\frac{kA_y}{\Delta y}\frac{\rho_s k_{rs}}{\mu_s}h_s\right]_{i+\frac{1}{2}\eta}\left(P_{i+\eta}^{n+1}-P_i^{n+1}\right)-\left[\frac{kA_y}{\Delta y}\frac{\rho_s k_{rs}}{\mu_s}h_s\right]_{i-\frac{1}{2}\eta}\left(P_i^{n+1}-P_{i-\eta}^{n+1}\right)$$

$$+\left[\frac{kA_y}{\Delta y}\frac{\rho_w k_{rw}}{\mu_w}h_w\right]_{i+\frac{1}{2}\eta}\left(P_{i+\eta}^{n+1}-P_i^{n+1}\right)-\left[\frac{kA_y}{\Delta y}\frac{\rho_s k_{rs}}{\mu_w}h_w\right]_{i-\frac{1}{2}\eta}\left(P_i^{n+1}-P_{i-\eta}^{n+1}\right)$$

$$+\left[\frac{A_x K_m}{\Delta x}\left(\frac{\partial T}{\partial P}\right)_h\right]_{i+\frac{1}{2}}\left(P_{i+1}^{n+1}-P_i^{n+1}\right)-\left[\frac{A_x K_m}{\Delta x}\left(\frac{\partial T}{\partial P}\right)_h\right]_{i-\frac{1}{2}}\left(P_i^{n+1}-P_{i-1}^{n+1}\right)$$

$$+\left[\frac{A_x K_m}{\Delta x}\left(\frac{\partial T}{\partial h}\right)_P\right]_{i+\frac{1}{2}}\left(h_{i+1}^{n+1}-h_i^{n+1}\right)-\left[\frac{A_x K_m}{\Delta x}\left(\frac{\partial T}{\partial h}\right)_P\right]_{i-\frac{1}{2}}\left(h_i^{n+1}-h_{i-1}^{n+1}\right)$$

$$+\left[\frac{A_y K_m}{\Delta y}\left(\frac{\partial T}{\partial P}\right)_h\right]_{i+\frac{1}{2}\eta}\left(P_{i+\eta}^{n+1}-P_i^{n+1}\right)-\left[\frac{A_y K_m}{\Delta y}\left(\frac{\partial T}{\partial P}\right)_h\right]_{i-\frac{1}{2}\eta}\left(P_i^{n+1}-P_{i-\eta}^{n+1}\right)$$

$$+\left[\frac{A_y K_m}{\Delta y}\left(\frac{\partial T}{\partial h}\right)_P\right]_{i+\frac{1}{2}\eta}\left(h_{i+\eta}^{n+1}-h_i^{n+1}\right)-\left[\frac{A_y K_m}{\Delta y}\left(\frac{\partial T}{\partial h}\right)_P\right]_{i-\frac{1}{2}\eta}\left(h_i^{n+1}-h_{i-\eta}^{n+1}\right)$$

$$+ V (q_s h_s + q_w h_w)$$

$$= \frac{\{V [\phi\rho h + (1 - \phi)\rho_r h_r]\}^{n+1} - V [\phi\rho h + (1 - \phi)\rho_r h_r]^n}{\Delta t} \quad (53)$$

$$\text{Let } E = V [\phi\rho h + (1 - \phi)\rho_r h_r], \quad (54)$$

$$q_h = q_s h_s + q_w h_w \quad (55)$$

and define the following interblock transmissibility terms:

$$T_{hx} = T_{wx} h_{wx} + T_{sx} h_{sx} + \left(\frac{A_x K_m}{\Delta x} \right) \left(\frac{\partial T}{\partial P} \right)_h \quad (56)$$

$$T_{hy} = T_{wy} h_{wy} + T_{sx} h_{sy} + \left(\frac{A_y K_m}{\Delta y} \right) \left(\frac{\partial T}{\partial P} \right)_h \quad (57)$$

$$T_{cx} = \left(\frac{A_x K_m}{\Delta x} \right) \left(\frac{\partial T}{\partial h} \right)_P \quad (58)$$

$$T_{cy} = \left(\frac{A_y K_m}{\Delta y} \right) \left(\frac{\partial T}{\partial h} \right)_P \quad (59)$$

With these and eqs. (45), (46), (47), (48), (54), (55), eq. (53) can be expressed as:

$$\Delta_x (T_{hx} \Delta_x p^{n+1}) + \Delta_y (T_{hy} \Delta_y p^{n+1})$$

$$+ \Delta_x (T_{cx} \Delta_x h^{n+1}) + \Delta_y (T_{cy} \Delta_y h^{n+1})$$

$$+ V q_h = \frac{E^{n+1} - E^n}{\Delta t} \quad (60)$$

where

$$\Delta_x(T_{hx}\Delta_x p^{n+1}) = T_{hx_{i+\frac{1}{2}}} (p_{i+1}^{n+1} - p_i^{n+1}) - T_{hx_{i-\frac{1}{2}}} (p_i^{n+1} - p_{i-1}^{n+1}) \quad (61)$$

$$\Delta_y(T_{hy}\Delta_y p^{n+1}) = T_{hy_{i+\frac{1}{2}\eta}} (p_{i+\eta}^{n+1} - p_i^{n+1}) - T_{hy_{i-\frac{1}{2}\eta}} (p_i^{n+1} - p_{i-\eta}^{n+1}) \quad (62)$$

Similar difference operations hold for T_{cx} and T_{cy} .

Eqs. (49) and (60) represent the finite difference analog of eqs. (1) and (2) respectively in concise form. Note that these two difference equations are formulated in fully implicit scheme.

Also, $M = M(P,h)$ (63)

$$\text{so} \quad dM = \frac{\partial M}{\partial P} dP + \frac{\partial M}{\partial h} dh \quad (64)$$

$$\text{or } M^{n+1} - M^n = \left(\frac{\partial M}{\partial P} \right)_{n+1} (P^{n+1} - P^n) + \left(\frac{\partial M}{\partial h} \right)_{n+1} (h^{n+1} - h^n) \quad (65)$$

$$E = E(P,h) \quad (66)$$

$$dE = \frac{\partial E}{\partial P} dP + \frac{\partial E}{\partial h} dh \quad (67)$$

$$\text{or} \quad E^{n+1} - E^n = \left(\frac{\partial E}{\partial P} \right)_{n+1} (P^{n+1} - P^n)$$

$$+ \left(\frac{\partial E}{\partial h}\right)_{n+1} \left(h^{n+1} - h^{n} \right) \qquad (68)$$

Using eqs. (65) and (68), eqs. (49) and (60) can be expressed respectively as:

$$\Delta_x \left[\left(T_{wx} + T_{sx} \right) \Delta_x p^{n+1} \right] + \Delta_y \left[\left(T_{wy} + T_{sy} \right) \Delta_y p^{n+1} \right]$$

$$+ Vq_t = \left(\frac{\partial M}{\partial P} \right)_{n+1} \frac{p^{n+1} - p^{n}}{\Delta t} +$$

$$\left(\frac{\partial M}{\partial h} \right)_{n+1} \frac{h^{n+1} - h^{n}}{\Delta t} \qquad (69)$$

$$\Delta_x \left(T_{hx} \Delta_x p^{n+1} \right) + \Delta_y \left(T_{hy} \Delta_y p^{n+1} \right)$$

$$+ \Delta_x \left(T_{cx} \Delta_x h^{n+1} \right) + \Delta_y \left(T_{cy} \Delta_y h^{n+1} \right)$$

$$+ Vq_h = \left(\frac{\partial E}{\partial P} \right)_{n+1} \frac{\left(p^{n+1} - p^{n} \right)}{\Delta t} + \left(\frac{\partial E}{\partial h} \right)_{n+1} \frac{\left(h^{n+1} - h^{n} \right)}{\Delta t} \qquad (70)$$

The boundary conditions given by eq. (3) to eq. (6) indicate a thermally insulated or a no-flow or an adiabatic geothermal reservoir boundary. The finite difference analog for these equations can be represented by the following equations:

$$P_i - P_{i-1} = 0 \qquad (71)$$

$$P_i - P_{i+1} = 0 \qquad (72)$$

$$h_i - h_{i-1} = 0 \qquad (73)$$

$$h_i - h_{i+1} = 0 \qquad (74)$$

$$P_i - P_{i-\eta} = 0 \qquad (75)$$

$$P_i - P_{i+\eta} = 0 \qquad (76)$$

$$h_i - h_{i-\eta} = 0 \qquad (77)$$

$$h_i - h_{i+\eta} = 0 \qquad (78)$$

Note that eq. (71) to eq. (78) correspond to zero transmissibility terms in the coefficients of the finite difference model eqs. (69) and (70) at the boundaries of the grid cells.

2.4 Solution Method

The transformation of the two continuous differential eqs. (1) and (2) into the two discrete difference eqs. (69) and (70) has been developed in the previous section. The solution of eqs. (69) and (70), with appropriate initial and boundary conditions of the geothermal system under concern will give pressure and enthalpy distributions versus time.

One common and direct approach of solving eqs. (69) and (70) is to solve them simultaneously by using some iterative technique as the coefficients in the difference equations are nonlinear. One such popular scheme is the Newton-Raphson method.

Note that for each cell in the reservoir grid there are two unknown variables P and h to be determined. Thus, there are five

unknowns for each equation and a total of ten unknowns for the two simultaneous eqs. (69) and (70) written for each cell. For a reservoir grid of N active cells, this would mean 2XN equations with 2XN unknowns to be computed.

The amount of computational work involved in solving eqs. (69) and (70) can be very large by using the aforementioned implicit simultaneous scheme especially if the reservoir grid is very large, e.g. a 400-cell grid. One approach to tackle this problem is to solve the finite difference eqs. (69) and (70) in sequence each time step (18). An example of sequential numerical solution is the " leapfrog " method (19) for solving average pressure and capillary pressure in sequence in petroleum reservoir simulation.

The solution method used in this study for solving eqs. (69) and (70), the finite difference analog, is based upon a variation of the sequential numerical solution. The complete algorithm is as follows:

Eq. (69) can be arranged to yield:

$$\Delta_x\left[\left(T_{wx} + T_{sx} \right) \Delta_x P^{n+1}\right] + \Delta_y\left[\left(T_{wy} + T_{sy} \right) \Delta_y P^{n+1} \right]$$

$$+ Vq_t - \frac{1}{\Delta t} \left[\left(\frac{\partial M}{\partial P} \right)_{n+1} P^{n+1} \right]$$

$$= - \frac{1}{\Delta t} \left[\left(\frac{\partial M}{\partial P} \right)_{n+1} \left(P^n \right) + \left(\frac{\partial M}{\partial h} \right)_{n+1} \left(h^{n+1} - h^n \right) \right] \qquad (79)$$

By using eqs. (50) and (51) and on collecting terms, eq. (79) can be written in compact form as:

$$e_{pi}P_{i-\eta}^{n+1} + a_{pi}P_{i-1}^{n+1} + b_{pi}P_{i}^{n+1} + c_{pi}P_{i+1}^{n+1} + f_{pi}P_{i+\eta}^{n+1} = d_{pi} \qquad (80)$$

with

$$e_{pi} = T_{wy_{i-\frac{1}{2}\eta}} + T_{sy_{i-\frac{1}{2}\eta}} \qquad (81)$$

$$a_{pi} = T_{wx_{i-\frac{1}{2}}} + T_{sx_{i-\frac{1}{2}}} \qquad (82)$$

$$b_{pi} = -\left[T_{wx_{i+\frac{1}{2}}} + T_{wx_{i-\frac{1}{2}}} + T_{sx_{i+\frac{1}{2}}} + T_{sx_{i-\frac{1}{2}}} + T_{wy_{i+\frac{1}{2}\eta}} + T_{wy_{i-\frac{1}{2}\eta}} + T_{sy_{i+\frac{1}{2}\eta}} + T_{sy_{i-\frac{1}{2}\eta}} + \frac{1}{\Delta t}\left(\frac{\partial M}{\partial P}\right)_{n+1}\right] \qquad (83)$$

$$c_{pi} = T_{wx_{i+\frac{1}{2}}} + T_{sx_{i+\frac{1}{2}}} \qquad (84)$$

$$f_{pi} = T_{wy_{i+\frac{1}{2}\eta}} + T_{sy_{i+\frac{1}{2}\eta}} \qquad (85)$$

$$d_{pi} = -\frac{1}{\Delta t}\left[\left(\frac{\partial M}{\partial P}\right)_{n+1} P_i^n + \left(\frac{\partial M}{\partial h}\right)_{n+1}\left(h_i^{n+1} - h_i^n\right)\right] - Vq_t \qquad (86)$$

Recall that the transmissibility terms are given by eqs. (45), (46), (47) and (48).

Similar to the above procedure, eq. (70) can be arranged as:

$$\Delta_x\left(T_{cx}\Delta_x h^{n+1}\right) + \Delta_y\left(T_{cy}\Delta_y h^{n+1}\right) + Vq_h - \frac{1}{\Delta t}\left[\left(\frac{\partial E}{\partial h}\right)_{n+1}\left(h^{n+1}\right)\right] =$$

$$-\Delta_x \left(T_{hx}\Delta_x p^{n+1} \right) - \Delta_y \left(T_{hy}\Delta_y p^{n+1} \right) + \frac{1}{\Delta t} \left[\left(\frac{\partial E}{\partial P} \right)_{n+1} \left(p^{n+1} - p^n \right) \right]$$

$$- \frac{1}{\Delta t} \left[\left(\frac{\partial E}{\partial h} \right)_{n+1} \left(h^n \right) \right] \qquad (87)$$

As before, eq. (87) can be written in compact form as:

$$e_{hi} h_{i-\eta}^{n+1} + a_{hi} h_{i-1}^{n+1} + b_{hi} h_i^{n+1} + c_{hi} h_{i+1}^{n+1} + f_{hi} h_{i+\eta}^{n+1} = d_{hi} \qquad (88)$$

with

$$e_{hi} = T_{cy_{i-\frac{1}{2}\eta}} \qquad (89)$$

$$a_{hi} = T_{cx_{i-\frac{1}{2}}} \qquad (90)$$

$$b_{hi} = - \left[T_{cx_{i+\frac{1}{2}}} + T_{cx_{i-\frac{1}{2}}} + T_{cy_{i+\frac{1}{2}\eta}} + T_{cy_{i-\frac{1}{2}\eta}} + \frac{1}{\Delta t} \left(\frac{\partial E}{\partial h} \right)_{n+1} \right] \qquad (91)$$

$$c_{hi} = T_{cx_{i+\frac{1}{2}}} \qquad (92)$$

$$f_{hi} = T_{cy_{i+\frac{1}{2}\eta}} \qquad (93)$$

$$d_{hi} = - \left(T_{hy_{i-\frac{1}{2}\eta}} \right) p_{i-\eta}^{n+1} - \left(T_{hx_{i-\frac{1}{2}}} \right) p_{i-1}^{n+1} +$$

$$\left[T_{hx_{i+\frac{1}{2}}} + T_{hx_{i-\frac{1}{2}}} + T_{hy_{i+\frac{1}{2}\eta}} + T_{hy_{i-\frac{1}{2}\eta}} + \frac{1}{\Delta t} \left(\frac{\partial E}{\partial P} \right) \right]_{n+1} p_i^{n+1}$$

$$- \left(T_{hx_{i+\frac{1}{2}}} \right) p_{i+1}^{n+1} - \left(T_{hy_{i+\frac{1}{2}\eta}} \right) p_{i+\eta}^{n+1}$$

$$- \frac{1}{\Delta t} \left(\frac{\partial E}{\partial P} \right)_{n+1} p_i^n - Vq_h - \frac{1}{\Delta t} \left[\left(\frac{\partial E}{\partial h} \right)_{n+1} \left(h_i^n \right) \right] \qquad (94)$$

Recall again the transmissibility terms are given by eqs. (45), (46), (47), (48), (56), (57), (58) and (59).

Eqs. (80) and (88) are just rearrangements of eqs. (69) and (70). Nothing new is created. However, these rearrangements permit the application of sequential method described earlier. Thus, at a certain time step, if the fluid enthalpy h is known at each cell, then the fluid pressure P at each cell can be computed by solving eq. (80). Once the P values are obtained, eq. (88) is then solved to back calculate or ' update ' h. The alternative to this is by first solving h using eq. (88) and then P by eq. (80). Hence, instead of solving eqs. (69) and (70) simultaneously (two unknowns in each grid cell), we end up solving two difference eqs. (80) and (88) one at a time (one unknown in each cell). It is obvious that solving eq. (80) or (88) is a lot easier than that of eqs. (69) and (70) simultaneously. More importantly, the former approach would be a more computationally efficient one than the latter scheme. Now it remains to decide which equation should be solved first in the simulation of geothermal reservoir: the pressure (or flow) eq. (80) or the enthalpy (or energy) eq. (88). The understanding of the thermodynamic properties of the geothermal fluid is important for doing this as well as giving physical support for the application of sequential scheme in geothermal reservoir simulation.

Consider fig. 1, the pressure-enthalpy diagram for compound water, showing three regions representing possible initial conditions for a geothermal reservoir.

If a reservoir were found that initially existed entirely within the compressed-water region ① , the producing mechanism

is likely to be due to the volumetric expansion of geothermal fluid as in the case of undersaturated oil reservoir production. Because of the immense amount of heat energy contained in the rock, the geothermal reservoir would be producing isothermally. Thus, according to fig. 1, this reservoir would follow an isoenthalpic path of production. In other words, on production, there would be a decrease in fluid pressure but only a slight or no change in fluid enthalpy. The simulation of this type of reservoir would allow us to solve for the flow equation first and then the energy equation later.

If a reservoir were found that initially existed entirely within the two-phase steam-water region ② , the reservoir could be produced in different ways (3). Two most possible schemes are discussed below. The first is that the reservoir can be produced isothermally, leading to a constant geothermal fluid pressure with a change in fluid enthalpy. The pressure starts to drop when all the liquid water has vaporized into steam. The simulation of this type of reservoir would allow us to solve for the enthalpy equation first and then the pressure equation later. The second is that the reservoir can be produced following an isoenthalpic path, resulting in both pressure and temperature decline. The simulation of this type of reservoir would allow us to solve for the pressure equation first and then the enthalpy equation later. For the two producing behavior discussed, the first one is the most likely to occur.

If a reservoir were found that initially existed entirely within the superheated-steam region ③ , the producing mechanism is likely to be due to the volumetric expansion of geothermal fluid

as in the case of dry hydrocarbon gas reservoir production. As in the case of compressed-water type reservoir, this reservoir would produce following an isothermal path (3), resulting in both pressure and enthalpy decline of the geothermal fluid. However, as indicated by fig. 1, the rate of change of fluid enthalpy would be a lot smaller than that of fluid pressure. The simulation of this type of reservoir would allow us to solve for the flow equation first and then the energy equation later.

In this study, the coefficients on the left side of eq. (80) or (88), involve terms which are dependent on P and h, are to be computed at the n+1 time level.

Consider the simulation of a compressed-water type geothermal reservoir using sequential method as described before. The procedures for solving the pressure and enthalpy equations are:

1. Assume $P^{n+1,k}$, $h^{n+1,k}$.
2. Compute coefficients of pressure eq. (80).
3. Solve eq. (80) to get $P^{n+1,k+1}$
4. Test for convergence:

$$\left| \frac{P^{n+1,k+1} - P^{n+1,k}}{P^{n+1,k}} \right| \leqslant \varepsilon \ ?$$

If convergence is attained, go to the next step.

If convergence is not attained, perform relaxation:

$$P^{n+1,k+1} = P^{n+1,k} + \omega_p \left(P^{n+1,k+1} - P^{n+1,k} \right), \text{ then}$$

repeat 2, 3 and 4.

5. Compute coefficients of enthalpy eq. (88)

6. Solve eq. (88) to get $h^{n+1,k+1}$

7. Test for convergence:

$$\left| \frac{h^{n+1,k+1} - h^{n+1,k}}{h^{n+1,k}} \right| \leqslant \varepsilon \ ?$$

If convergence is attained, go to the next step.

If convergence is not attained, perform relaxation:

$h^{n+1,k+1} = h^{n+1,k} + \omega_h (h^{n+1,k+1} - h^{n+1,k})$, then repeat 5, 6 and 7.

8. Use linear interpolation to predict the $P^{n+1,k}$,$h^{n+1,k}$ values of the next time step. Repeat 2,3,...,8.

The above process can be summarized in the following flowchart. The one for first solving eq. (88) and then eq. (80) is similar.

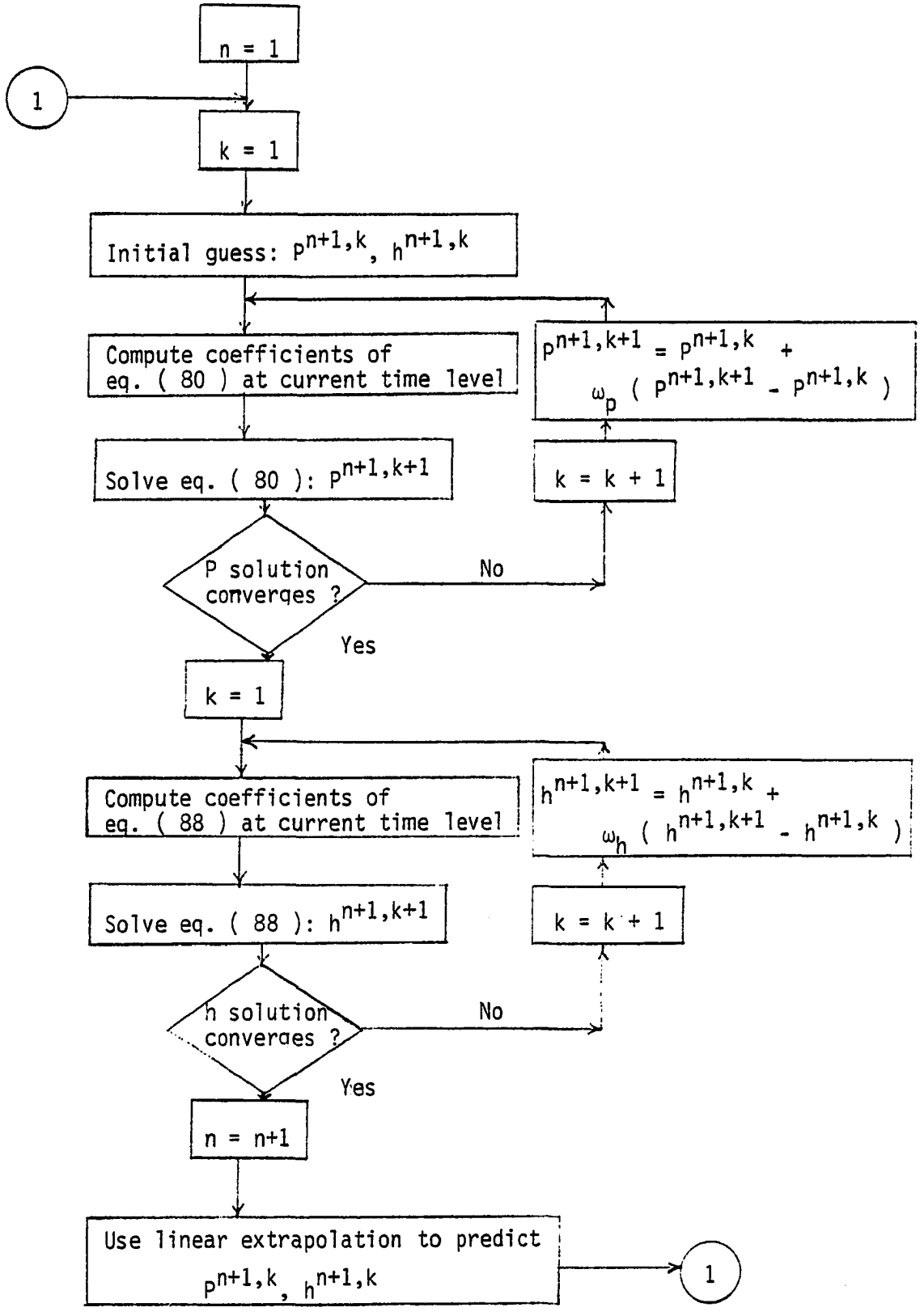

Fig. 5 Flowchart: main algorithm for solving pressure and enthalpy equations sequentially

The previous discussion of the use of sequential solution technique in geothermal reservoir simulation is based on the fact that the geothermal reservoir is either in the compressed-water region, the steam-water region, or the superheated-steam region. If the reservoir is in the period of transition from one region to another region during simulation, the sequential technique can be used by utilizing a smaller time step to minimize mathematical truncation errors. Once the reservoir has been switched completely to a ' new ' region, the methods discussed before can be used. For instance, a geothermal reservoir is initially in the compressed-water region ① of fig. 1; it is to be produced isothermally. Thus the flow equation will be solved first; the energy equation will then be solved to back calculate enthalpy. During the time the reservoir is changing from compressed-water type to two-phase steam-water type, a smaller time step is used, still solving flow equation first and energy equation second. Once the whole reservoir is in the steam-water region, the simulation will proceed with solving energy equation first and flow equation later as the reservoir is to be produced isothermally.

2.5 Matrix Solution Mehtod: SIP

Eq. (80) or (88) when written for each active cell in a reservoir grid of N active cells will produce a system of pentadiagonal matrix equations to be solved:

$$\begin{bmatrix} & & & f_{pi} & \\ & & c_{pi} & & \\ & b_{pi} & & & \\ a_{pi} & & & & \\ & e_{pi} & & & \end{bmatrix} \begin{bmatrix} P_1 \\ \vdots \\ P_i \\ \vdots \\ P_N \end{bmatrix} = \begin{bmatrix} d_{p1} \\ \vdots \\ d_{pi} \\ \vdots \\ d_{pN} \end{bmatrix} \qquad (95)$$

$$\begin{bmatrix} & & & f_{hi} & \\ & & c_{hi} & & \\ & b_{hi} & & & \\ a_{hi} & & & & \\ & e_{hi} & & & \end{bmatrix} \begin{bmatrix} h_1 \\ \vdots \\ h_i \\ \vdots \\ h_N \end{bmatrix} = \begin{bmatrix} d_{h1} \\ \vdots \\ d_{hi} \\ \vdots \\ d_{hN} \end{bmatrix} \qquad (96)$$

The selection of a method to solve the above pentadiagonal matrix system is very important because the efficiency of a reservoir simulator is determined by its ability to solve the pressure (or enthalpy in this case) equations efficiently (17). The choice of either direct or iterative method, which are the two main matrix solution methods, to solve a matrix system, is based chiefly on the size, the sparseness and the diagonal dominance of the matrix system. Generally speaking, direct methods like matrix decomposition (LUD), Gauss-Jordan, etc. are adequate for full small matrices (e.g.less than 50 x 50 system). Iterative methods like Gauss-Seidel, relaxation,etc. are good for large sparse matrices (e.g. a 400 x 400 system). In this study, an iterative scheme is used in the geothermal reservoir simulator. The main reason is that

the simulator is designed to be capable of handling a large reservoir grid.

Among the different iterative methods for solving pentadiagonal matrix systems in petroleum reservoir simulation,

PSOR (point successive overrelaxation),

LSOR (line successive overrelaxation),

ADIP (alternative direction implicit procedure), and

SIP (strongly implicit procedure)

are the most common ones to be used. In this study, SIP is implemented in solving the pressure or enthalpy equations for the following reasons.

First, SIP is applicable to both heterogeneous and anisotropic reservoirs, which are the more realistic ones (instead of homogeneous and isotropic types) found . Second, SIP is not very sensitive to the selection of its iteration parameters, which makes the iterative method simple to use. Third, SIP usually converges faster than other methods except in the trivial case of solving homogeneous and isotropic systems. Details of comparision of SIP with other competitive matrix methods can be found in Stone (20) and Weinstein (21).

There are three versions of SIP, namely, odd-numbered iteration, even-numbered iteration and odd-even-numbered iteration. The last version is determined to be the best by Suarez and Farouq Ali (22). Thus the odd-even-numbered iteration will be used in this study. The complete algorithm and the selection of iteration parameters are well documented in Stone (20), Weinstein (21) and Al-Marhoun (23). They are summarized as the following (17,23) :

Consider the following equation written for a cell in fig. 4:

$$e_i x_{i-\eta} + a_i x_{i-1} + b_i x_i + c_i x_{i+1} + f_i x_{i+\eta} = d_i \qquad (97)$$

This equation when written for every cell in a reservoir grid of N active cells will produce a system of pentadiagonal matrix equations to be solved:

$$\begin{bmatrix} & & & & f_i \\ & & & & \\ & & & & \\ & a_i & & & \\ & & b_i & & \\ & & & c_i & \\ e_i & & & & \end{bmatrix} \begin{bmatrix} x_1 \\ \vdots \\ x_i \\ \vdots \\ x_N \end{bmatrix} = \begin{bmatrix} d_1 \\ \vdots \\ d_i \\ \vdots \\ d_N \end{bmatrix} \qquad (98)$$

or equivalently:

$$AX = D \qquad (99)$$

SIP, an iterative scheme, involves the transformation of the original pentadiagonal matrix A into a modified matrix A' which can be easily factorized into a product of of two matrices: the lower triangular matrix L and the upper triangular matrix U.

Define

$$\delta^{k+1} = x^{k+1} - x^k \qquad (100)$$

$$R^k = D - AX^k \qquad (101)$$

Solving the original eq. (99) is equivalent to solving:

$$A'\delta^{k+1} = R^k \qquad (102)$$

$$\text{As} \quad A' = LU \qquad (103)$$

eq. (102) becomes

$$LU\delta^{k+1} = R^k \qquad (104)$$

let

$$v^{k+1} = U\delta^{k+1} \qquad (105)$$

$$\text{so} \quad Lv^{k+1} = R^k \qquad (106)$$

$$\text{and} \quad U\delta^{k+1} = v^{k+1} \qquad (107)$$

v^{k+1} and δ^{k+1} can be solved very easily by performing forward and backward substitutions on eqs. (106) and (107) respectively. The unknown vector x is then computed as:

$$x^{k+1} = x^k + \delta^{k+1} \qquad (108)$$

Convergence of the solution is reached when the following is satisfied:

$$r_i = \left| \frac{x_i^{k+1} - x_i^k}{x_i^{k+1}} \right| \leqslant \varepsilon \ , \qquad (109)$$

$i = 1,2,\ldots,N$.

ε, a predetermined error tolerance.

In the odd-numbered iterations, the L and U are:

$$L = \begin{bmatrix} & & & \\ & A_i & & \\ & & B_i & \\ E_i & & & \end{bmatrix} \qquad (110)$$

$$U = \begin{bmatrix} & & & F_i \\ & & C_i & \\ & 1 & & \\ & & & \end{bmatrix} \qquad (111)$$

The factorization algorithm for $i = 1,2,\ldots,N$ is

$$g_i = e_i C_{i-n} / (\alpha_r C_{i-n} + 1) \qquad (112)$$

$$h_i = a_i F_{i-1} / (\alpha_r F_{i-1} + 1) \qquad (113)$$

$$E_i = e_i - \alpha_r g_i \qquad (114)$$

$$A_i = a_i - \alpha_r h_i \qquad (115)$$

$$B_i = b_i + \alpha_r g_i + \alpha_r h_i - E_i F_{i-\eta} - A_i C_{i-1} \qquad (116)$$

$$C_i = (c_i - \alpha_r g_i) / B_i \qquad (117)$$

$$F_i = (f_i - \alpha_r h_i) / B_i \qquad (118)$$

where α_r is the SIP iteration parameter.

Once the L and U coefficients are computed,

$$v_i^{k+1} = (R_i^k - E_i v_{i-\eta}^{k+1} - A_i v_{i-1}^{k+1}) / B_i \ , \qquad (119)$$

$$i = 1,2,\ldots,N.$$

and

$$\delta_i^{k+1} = v_i^{k+1} - C_i \delta_{i+1}^{k+1} - F_i \delta_{i+\eta}^{k+1} \ , \qquad (120)$$

$$i = N,N-1,\ldots,1.$$

In the even-numbered iteration, the L and U are:

$L =$ 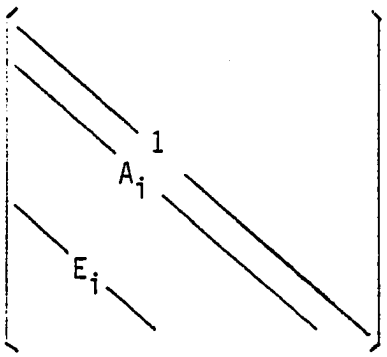

(121)

$U =$ 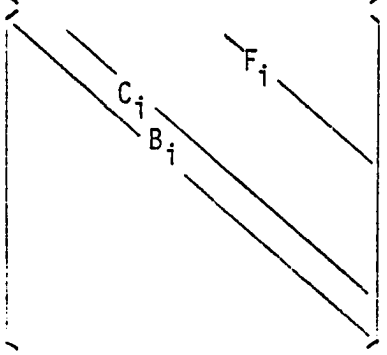

(122)

The factorization algorithm for i = N,N-1,...,1 is

$$g_i = c_i E_{i+1} / (\alpha_r E_{i+1} + 1) \qquad (123)$$

$$h_i = f_i A_{i+\eta} / (\alpha_r A_{i+\eta} + 1) \qquad (124)$$

$$F_i = f_i - \alpha_r h_i \qquad (125)$$

$$C_i = c_i - \alpha_r g_i \qquad (126)$$

$$B_i = b_i + \alpha_r g_i + \alpha_r h_i - C_i A_{i+1} - F_i E_{i+\eta} \qquad (127)$$

$$A_i = (a_i - \alpha_r h_i) / B_i \qquad (128)$$

$$E_i = (e_i - \alpha_r g_i) / B_i \qquad (129)$$

where α_r is the SIP iteration parameter.

Once the L and U coefficients are computed,

$$v_i^{k+1} = (R_i - C_i v_{i+1} - F_i v_{i+\eta}) / B_i , \qquad (130)$$

$$i = N, N-1, \ldots, 1.$$

and

$$\delta^{k+1} = v_i^{k+1} - E_i \delta_{i-\eta}^{k+1} - A_i \delta_{i-1}^{k+1} , \qquad (131)$$

$$i = 1, 2, \ldots, N.$$

Thus the odd-even-numbered version of SIP is made up of a sequence of operations of odd-iteration followed by even-iteration described above.

The SIP iteration parameters α_r are given by (18):

$$1 - \alpha_{max} = \min_{ij} \left[\frac{\pi^2}{2I^2 (1+AY/AX)}, \frac{\pi^2}{2J^2 (1+AX/AY)} \right] , \qquad (132)$$

$$1 - \alpha_r = (1 - \alpha_{max})^{(r-1)/(s - 1)} , \qquad (133)$$

where AY = transmissibility in y-direction,

AX = transmissibility in x-direction,

s = number of parameters in the cycle

and each α_r is used twice in succession (odd-even-iteration).

2.6 Computer Geothermal Simulator: CGS

Based upon the previous discussions, an efficient geothermal reservoir simulator using the sequential technique can be implemented. The computer geothermal simulator developed in this study, entitled CGS , is a two-dimensional (x-y) simulator capable of simulating either one-phase or two-phase, homogeneous or heterogeneous, isotropic or anisotropic geothermal reservoir systems with sinks and sources included (if any). The computational units used in the simulator are the centimeter-gram-second (CGS)units. However, input and output units can be in terms of petroleum engineering field units.

CGS is coded in FORTRAN IV language and is made up of one main program and 24 subroutines. Every effort is made to program the simulator (CGS) in the most efficient way. The concepts of structured programming are used: GO-TO less programming, modularization of programs, and the top-down design of programs (24). Unnecessary and redundant computer statements are avoided. CGS is debugged on the IBM 370/158 computer. The design of the main program is presented in this section while the different subroutines with the affiliated algorithms are presented in the following section. For better and clearer presentation, a pseudo language is used instead of flowcharts for describing the different routines in CGS (25).

PSUEDO LANGUAGE DESCRIPTION OF COMPUTER GEOTHERMAL SIMULATOR (CGS)

MAIN

ASSIGN ARRAY AREA FOR VARIABLES

INITIALIZE DATA

READ WELL INFORMATION

CALL TITLE: TO IDENTIFY THE SIMULATION RUN

CALL GRID: TO INPUT RESERVOIR GRID INFORMATION

CALL CELL: TO IDENTIFY ACTIVE CELLS

CALL INPUT: TO INPUT $\Delta x, \Delta y$, b, k, ϕ, P_i, h_i, K_m, T_i

CALL OUTIN: TO OUTPUT THE ABOVE LIST OF VARIABLES

COMPUTE VOLUME OF EACH CELL, MASS IN PLACE, ENERGY IN PLACE,
WATER IN PLACE, STEAM IN PLACE

KODE = 0

INITIALIZE h^n, $h^{n+1,k}$, P^n, $P^{n+1,k}$, T^n

CALL CONTER: TO COMPUTE THE CONSTANT TERMS IN SIMULATION

TIME = 0

START DO

TIME = TIME + DT

IF (TIME .LE. FINTIM) THEN

1 CALL HSHW: TO FIND h_s, h_w

CALL FUNPHA: TO DETERMINE THE PHASE STATUS OF EACH ACTIVE CELL,
THE RESERVOIR TYPE, ITYPE (1 FOR 1-P, 2 FOR 2-P), AND
S_w, S_s, k_{rw}, k_{rs}, T, μ_w, μ_s, ρ, ρ_w, ρ_s, $\left(\frac{\partial T}{\partial P}\right)_h$, $\left(\frac{\partial T}{\partial h}\right)_P$

2 CALL POR: TO COMPUTE ROCK POROSITY

CALL ROCKH: TO COMPUTE ROCK ENTHALPY

CALL WELL: TO COMPUTE FLUID AND ENERGY FLOW RATE IN WELLS

CALL UPSTRM: TO 'UPSTREAM WEIGH' EACH INTERBLOCK h_w, h_s, k_{rw}, k_{rs}

CALL METDER: TO COMPUTE $\frac{\partial M}{\partial P}$, $\frac{\partial M}{\partial h}$, $\frac{\partial E}{\partial P}$, $\frac{\partial E}{\partial h}$

CALL TRANSM: TO COMPUTE TRANSMISSIBILITY TERMS T_w, T_s, T_h, T_c

IF (ITYPE .EQ. 2) GOTO4

IF (KODE .NE. 1) THEN

3 CALL COEP: TO COMPUTE PRESSURE EQUATION COEFFICIENTS

CALL ALSIP: TO COMPUTE OPTIMUM SIP ITERATION PARAMETERS FOR PRESSURE EQUATION

CALL SIP: TO COMPUTE $P^{n+1,k+1}$ BY SIP

KODE = 0

TEST FOR CONVERGENCE OF P:

IF (CONVERGENCE .EQ. FALSE) THEN

CALL RELAX: $P^{k+1} = P^k + \omega_p(P^{k+1} - P^k)$

GOTO2

END IF

IF (ITYPE .EQ. 2) GOTO5

ELSE

4 CALL COEH: TO COMPUTE ENTHALPY EQUATION COEFFICIENTS

CALL ALSIP: TO COMPUTE OPTIMUM SIP ITERATION PARAMETERS FOR ENTHALPY EQUATION

CALL SIP: TO COMPUTE $h^{n+1,k+1}$ BY SIP

KODE = 1

TEST FOR CONVERGENCE OF h:

IF (CONVERGENCE .EQ. FALSE) THEN

CALL RELAX: $h^{k+1} = h^k + \omega_h(h^{k+1} - h^k)$

GOTO2

END IF

IF (ITYPE .EQ. 2) GOTO3

5 CALL MBC2: MATERIAL BALANCE CHECK, MBC

IF (MBC OK) THEN

CALL HSHW: TO FIND h_s, h_w

CALL FUNPHA: TO DETERMINE THE PHASE STATUS OF EACH ACTIVE CELL,

THE RESERVOIR TYPE, ITYPE (1 for 1-P, 2 for 2-P), AND

S_w, S_s, k_{rw}, k_{rs}, T, μ_w, μ_s, ρ, ρ_w, ρ_s, $\left(\frac{\partial T}{\partial P} \right)_h$, $\left(\frac{\partial T}{\partial h} \right)_P$

CALL RESULT: WRITE RESULTS, P, h, T, S_w

ELSE

ADJUST TIME STEP DT

GOTO1

END IF

RESET P^n, h^n, T^n

CALL PREDIH: TO PREDICT $P^{n+1,k}$, $h^{n+1,k}$

KODE = 0

ELSE

STOP SIMULATION

END IF

END DO

2.7 Simulator Subroutines

The subroutines implemented in CGS are presented in alphabetical order as the following.

Subroutine ALSIP

Purpose: to compute optimum SIP iteration parameters

Other subprograms required: none

The algorithm is given by eqs. (132) and (133).

PSEUDO LANGUAGE DESCRIPTION OF ALSIP:

SUBROUTINE ALSIP

ASSIGN ARRAY AREA FOR a, c, e, f, α

START DO: K = 1, M

COMPUTE α_{max}: EQ. (132)

END DO

START DO: I = 1, NPSIP

COMPUTE α_i: EQ. (133)

END DO

RETURN

Subroutine CELL

Purpose: to identify the active cells in the reservoir grid

Other subprograms required: OUTCEL

Regular Gaussian ordering of grid is used (18).

PSEUDO LANGUAGE DESCRIPTION OF CELL:

SUBROUTINE CELL

ASSIGN ARRAY AREA FOR ICELL, IACT, etc.

WRITE CELL INDEX IN GRID USING GAUSSIAN ORDERING

CALL OUTCEL

READ ICELL

IDENTIFY ICELL AS ACTIVE (1) OR INACTIVE (0)

COUNT THE NO. OF ACTIVE CELLS, M

CALL OUTCEL

RETURN

Subroutine COEH

Purpose: to compute the coefficients of enthalpy eq. (88)

Other subprograms required: none

PSEUDO LANGUAGE DESCRIPTION OF COEH:

SUBROUTINE COEH

ASSIGN ARRAY AREA FOR TRANSMISSIBILITY TERMS AND OTHERS

START DO: K = 1, M

i = ACTIVE CELL INDEX

COMPUTE

e_{hi} EQ. (89)

a_{hi} EQ. (90)

b_{hi} EQ. (91)

c_{hi} EQ. (92)

f_{hi} EQ. (93)

d_{hi} EQ. (94)

END DO

RETURN

Subroutine COEP

Purpose: to compute the coefficients of pressure eq. (80)

Other subprograms required: none

PSEUDO LANGUAGE DESCRIPTION OF COEP:

SUBROUTINE COEP

ASSIGN ARRAY AREA FOR TRANSMISSIBILITY TERMS AND OTHERS

START DO: K = 1,M

i = ACTIVE CELL INDEX

COMPUTE

e_{pi} EQ. (81)

a_{pi} Eq. (82)

b_{pi} EQ. (83)

c_{pi} EQ. (84)

f_{pi} EQ. (85)

d_{pi} EQ. (86)

END DO

RETURN

Subroutine CONTER

Purpose: to compute constant terms in simulation

Other subprograms required: none

In this routine, the absolute permeabilities k_x, k_y and thermal conductivities K_{mx}, K_{my} are harmonic weighted, Δx, Δy, and b mid-point weighted (18).

PSEUDO LANGUAGE DESCRIPTION OF CONTER:

SUBROUTINE CONTER

ASSIGN ARRAY AREA FOR k, Δx, Δy, b, K_m, etc.

START DO: K = 1, M

COMPUTE INTERBLOCK Δx, Δy, b, k_x, k_y ,K_{mx} , K_{my} , $kA/\Delta x$, $kA/\Delta y$

END DO

RETURN

Subroutine FUNPHA

Purpose: to determine the phase status of each active cell, the reservoir type, ITYPE (1 for 1-P, 2 for 2-P), and S_w, S_s, k_{rw}, k_{rs}, T, μ_w, μ_s, ρ, ρ_w, ρ_s, $\left(\frac{\partial T}{\partial P}\right)_h$, $\left(\frac{\partial T}{\partial h}\right)_P$

Other subprograms required: RELPER

The following equations (9) are used in this routine:

Refer to fiq. 1, the pressure-enthalpy diagram for compound water.

Define

$$p = \frac{P}{10^7} \qquad (134)$$

$$H = \frac{h}{10^7} \qquad (135)$$

where P = geothermal fluid pressure, dynes/cm^2,

h = geothermal fluid enthalpy, ergs/g

In the compressed-water region ① :

$$S_w = 1 \qquad (136)$$

$$S_s = 0 \qquad (137)$$

$$k_{rw} = 1 \qquad (138)$$

$$k_{rs} = 0 \qquad (139)$$

$$T = T_w (p,H)$$

$$= -28.1515 - 0.137458p + 0.301117H + 3536.37/H -$$

$$4.31919\times10^{-5}H^2 \qquad (140)$$

$$\mu_w = \mu_w(T)$$
$$= 10^{-6}\{241.4\times10^{[247.8/(T+133.15)]}\} \qquad (141)$$

$$\rho = \rho_w(p,H)$$
$$= 0.989875 + 4.00894\times10^{-4}p - 4.00489\times10^{-5}H + 2.66608/H$$

$$+ 5.46283\times10^{-7}pH - 1.29958\times10^{-7}H^2 \qquad (142)$$

In this study, $\left(\frac{\partial T}{\partial P}\right)_h$ can be obtained by differentiating eq. (140), so

$$\left(\frac{\partial T}{\partial P}\right)_h = \left(\frac{\partial T}{\partial p}\right)_H \left(\frac{\partial p}{\partial P}\right)$$
$$= -0.137458\times10^{-7} \qquad (143)$$

Similarly,

$$\left(\frac{\partial T}{\partial h}\right)_p = \left(\frac{\partial T}{\partial H}\right)_p \left(\frac{\partial H}{\partial h}\right)$$

$$= (0.301117 - 3536.37/H^2 - 8.63838\times10^{-5}H)\times10^{-7} \qquad (144)$$

In the superheated-syeam region ③ :

$$S_w = 0 \qquad (145)$$

$$S_s = 1 \qquad (146)$$

$$k_{rw} = 0 \qquad (147)$$

$$k_{rs} = 1 \qquad (148)$$

$$T = T_s(p,H)$$

$$= -374.669 + 47.9921p - 0.633606p^2 + 7.39386\times10^{-5}H^2$$

$$- 3.3372\times10^{6}/(H^2p^2) + 0.0357154/p^3 - 1.1725\times10^{-9}H^3p$$

$$- 2.26861\times10^{15}/H^4 \qquad (149)$$

$$\mu_s = \mu_s(T)$$

$$= 10^{-6}(0.407T + 80.4) \qquad (150)$$

$$\rho = \rho_s(p,H)$$

$$= -2.26162\times10^{-5} + 0.0438441p - 1.79088\times10^{-5}pH + 3.69276\times10^{-8}p^4$$

$$+ 5.17644\times10^{-13}H^3p \qquad (151)$$

As before,

$$\left(\frac{\partial T}{\partial P}\right)_h = \left(\frac{\partial T}{\partial p}\right)_H \left(\frac{\partial p}{\partial P}\right)$$

$$= \left[47.9921 - 1.267212p + 6.6744 \times 10^{6} / (H^{2} p^{3}) - 0.1071462/p^{4} \right.$$

$$\left. - 1.1725 \times 10^{-9} h^{3} \right] \times 10^{-7} \qquad (152)$$

$$\left(\frac{\partial T}{\partial h} \right)_{p} = \left(\frac{\partial T}{\partial H} \right)_{p} \left(\frac{\partial H}{\partial h} \right)$$

$$= \left[14.78772 \times 10^{-5} H + 6.6744 \times 10^{6} / (H^{3} p^{2}) \right.$$

$$\left. - 3.5175 \times 10^{-9} H^{2} p + 9.07444 \times 10^{15} / H^{5} \right] \times 10^{-7} \qquad (153)$$

In the water-steam region ② :

$$S_{w} = \frac{h - h_{s}}{h_{w} - h_{s}} \qquad (154)$$

and $$S_{s} = 1 - S_{w} \qquad (155)$$

where

$h_{s} = h_{s} (p)$, same as eq. (169) described in subroutine HSHW, (156)

$h_{w} = h_{w} (p)$, same as eq. (170) described in subroutine HSHW. (157)

k_{rw}, k_{rs} are obtained by calling the subroutine RELPER described later.

The following equation is developed using the temperature-pressure data for saturated steam (26).

$$T = T(P)$$

$$= 3.89878P^{0.237722} \qquad (158)$$

where T is in ^{o}C and P in dynes/cm^2.

$$\mu_w = \mu_w(T), \text{ same as eq. (141)} \qquad (159)$$

$$\mu_s = \mu_s(T), \text{ same as eq. (150)} \qquad (160)$$

$$\rho_w = \rho_w(p,H), \text{ same as eq. (142)} \qquad (161)$$

$$\rho_s = \rho_s(p,H), \text{ same as eq. (151)} \qquad (162)$$

$$\rho = \rho_w S_w + \rho_s S_s \qquad (163)$$

As before,

$$\left(\frac{\partial T}{\partial P}\right)_h = 0.926826P^{-0.762268} \qquad (164)$$

$$\left(\frac{\partial T}{\partial h}\right)_P = 0 \qquad (165)$$

The determination of the geothermal fluid phase (water, water-steam or steam) in an active cell i can be done by using the following inequalities:

if $h_i < h_{wi}$, fluid is compressed-water (one-phase) (166)

if $h_{wi} \leqslant h_i \leqslant h_{si}$, fluid is water-steam (two-phase) (167)

if $h_i > h_{si}$, fluid is superheated-steam (one-phase) (168)

h_w, h_s are the enthalpies of saturated water and steam respectively.

PSEUDO LANGUAGE DESCRIPTION OF FUNPHA :

ASSIGN ARRAY AREA FOR P, h, S_s, S_w, k_{rw}, k_{rs}, μ_w,μ_s, ρ, ρ_w, ρ_s, T, h_s, h_w, $\frac{\partial T}{\partial P}$, $\frac{\partial T}{\partial h}$, IPHASE, etc.

START DO: K = 1, M

i = ACTIVE CELL INDEX

DETERMINE FLUID PHASE IN EACH CELL i USING EQS. (166), (167), (168)

$IPHASE_i$ = 1 FOR COMPRESSED-WATER, 2 FOR WATER-STEAM, 3 FOR SUPERHEATED-STEAM

IF ($IPHASE_i$ .EQ. 1) THEN

COMPUTE S_w, S_s, k_{rw}, k_{rs}, T, μ_w, ρ, $(\frac{\partial T}{\partial P})_h$, $(\frac{\partial T}{\partial h})_P$ USING EQS. (136),...,(144)

END IF

IF ($IPHASE_i$ .EQ. 2) THEN

COMPUTE ρ_w,ρ_s, S_w, S_s USING EQ. (142) , EQ. (151) , EQS. (154),...,(157)

CALL RELPER: TO COMPUTE k_{rw}, k_{rs}

COMPUTE T, μ_w, μ_s, ρ, $(\frac{\partial T}{\partial P})_h$, $(\frac{\partial T}{\partial h})_P$ USING EQS. (158),...,(165)

END IF

IF ($IPHASE_i$ .EQ. 3) THEN

COMPUTE S_w, S_s, k_{rw}, k_{rs}, T, μ_s, ρ, $(\frac{\partial T}{\partial P})_h$, $(\frac{\partial T}{\partial h})_P$ USING EQS. (145),,,(153)

END IF

END DO

RETURN

Subroutine GRID

Purpose: to input reservoir grid information

Other subprograms required: none

PSEUDO LANGUAGE DESCRIPTION OF GRID:

SUBROUTINE GRID

READ I, J

N = I * J

RETURN

Subroutine HSHW

Purpose: to find h_s, h_w

Other subprograms required: none

The following correlation equations (9) for saturated steam and saturated water are used in this routine:

$$h_s = (2822.82 - 39.952/p + 2.54342/p^2 - 0.938879p^2) \times 10^7 \quad (169)$$

$$h_w = (809.674 + 94.4665p - 4.50247p^2 + 0.120265p^3 - 162.7/p + 29.8163/p^2 - 1.75623/p^3) \times 10^7 \quad (170)$$

where p is defined in eq. (134).

PSEUDO LANGUAGE DESCRIPTION OF HSHW :

SUBROUTINE HSHW

ASSIGN ARRAY AREA FOR h_s, h_w, P, etc.

START DO: K = 1, M

i = ACTIVE CELL INDEX

COMPUTE

h_{si} EQ. (169)

h_{wi} EQ. (170)

END DO

RETURN

Subroutine INPUT

Purpose: to input a matrix of grid variables

Other subprograms required: none

Input variables like Δx, Δy, k, P_i , etc. are read in the main program through the use of this routine. This routine can modify the given grid data (v) by adding (or subtracting) a constant (B) and/or multiplying a constant (A) to the original data to become v':

$$v' = Av + B \qquad (171)$$

PSEUDO LANGUAGE DESCRIPTION OF INPUT:

SUBROUTINE INPUT

ASSIGN ARRAY AREA FOR VAR, ID, etc.

READ ID

READ ICODE, SAME, A, B

IF (ICODE .EQ. 1) VAR_i = SAME: i = 1, M

READ VAR_i: i = 1, M

IF (ICODE .EQ. 2) RETURN

IF (ICODE .EQ. 3) VAR_i= A * VAR_i: i = 1, M

IF (ICODE .EQ. 4) VAR_i= VAR_i + B: i = 1, M

IF (ICODE .EQ. 5) VAR_i= A * VAR_i + B: i = 1, M

RETURN

Subroutiine MBC2

Purpose: to compute material balance error

Other subprograms required: none

The relative material balance errors for water and steam can be computed (23) as the following:

$$M_j = \sum_{i=1}^{N} \left[V\rho_j S_j - (q_{jc} + q_j \Delta t) \right]_i , \; j = w, s \qquad (172)$$

$$M_t = MIP_w + MIP_s \qquad (173)$$

$$r_j = \frac{1}{MIP_j} (M_j - MIP_j), \; j = w, s \qquad (174)$$

$$r_t = \frac{1}{M_t} (M_w + M_s - M_t) \qquad (175)$$

Define

$$r = \max \left| r_j \right| , \; j = w,s,t \qquad (176)$$

In order for a simulation model to be stable, we require

$$r \leqslant \varepsilon_m \qquad (177)$$

where ε_m is a predetermined error tolerance criterion.

When eq. (177) is satisfied or the number of trials of different time steps (Δt's) has been exceeded, the cumulative fluid and energy production for water and/or steam are updated as follows:

$$q_{wc}^{n+1} = q_{wc}^{n} + q_{w}^{n+1}\Delta t \qquad (178)$$

$$q_{sc}^{n+1} = q_{sc}^{n} + q_{s}^{n+1}\Delta t \qquad (179)$$

$$q_{hc}^{n+1} = q_{hc}^{n} + q_{h}^{n+1}\Delta t \qquad (180)$$

PSEUDO LANGUAGE DESCRIPTION OF MBC2:

SUBROUTINE MBC2

ASSIGN ARRAY AREA FOR ϕ, ρ_w, ρ_s, q_w, q_s, q_{wc}, q_{sc}, S_w, S_s, q_h, q_{hc}, etc.

SET W, S, RW, RS ALL ZERO

COMPUTE r_j, r_t, r USING EQS. (174),...,(176)

IF (r .LE. ε_m .OR. NTRIAL .GT. MAXDT) THEN

COMPUTE q_{wc}^{n+1} , q_{sc}^{n+1}, q_{hc}^{n+1} FOR EACH WELL USING EQS. (178),...,(180)

ELSE

RETURN

END IF

RETURN

Subroutine METDER:

Purpose: to compute $\frac{\partial M}{\partial P}$, $\frac{\partial M}{\partial h}$, $\frac{\partial E}{\partial P}$, $\frac{\partial E}{\partial h}$,

Other subprograms required: none

Recall

$$M = V\phi\rho \qquad (44)$$

$$E = V\left[\phi\rho h + (1 - \phi)\rho_r h_r\right] \qquad (54)$$

Using the first forward difference approximation, the following partial derivatives are obtained:

$$\frac{\partial M}{\partial P} = \frac{M^{n+1} - M^n}{\Delta P} \qquad (181)$$

$$\frac{\partial M}{\partial h} = \frac{M^{n+1} - M^n}{\Delta h} \qquad (182)$$

$$\frac{\partial E}{\partial P} = \frac{E^{n+1} - E^n}{\Delta P} \qquad (183)$$

$$\frac{\partial E}{\partial h} = \frac{E^{n+1} - E^n}{\Delta h} \qquad (184)$$

PSUEDO LANGUAGE DESCRIPTION OF METDER:

SUBROUTINE METDER

ASSIGN ARRAY AREA FOR $\frac{\partial M}{\partial P}$, $\frac{\partial M}{\partial h}$, $\frac{\partial E}{\partial P}$, $\frac{\partial E}{\partial h}$, etc.

START DO: K = 1, M

i = ACTIVE CELL INDEX

COMPUTE M^n , E^n USING EQS. (44), (54)

COMPUTE $\left(\frac{\partial M}{\partial P}\right)_i$, $\left(\frac{\partial M}{\partial h}\right)_i$, $\left(\frac{\partial E}{\partial P}\right)_i$, $\left(\frac{\partial E}{\partial h}\right)_i$ USING EQS. (181),...,(184)

END DO

RETURN

Subroutine OUTCEL

Purpose: to output a matrix of integer variables

Other subprograms required: none

This routine is used in the routine CELL for printing out the Gaussian ordering of the reservoir grid and the distributions of the active and inactive cells.

PSEUDO LANGUAGE DESCRIPTION OF OUTCEL:

```
SUBROUTINE OUTCEL
ASSIGN ARRAY AREA FOR KVA
START DO: K1 = 1, I, IW
K2 = MINO ( K1 + IW - 1, I )
START DO: K = 1, J
WRITE KVA (( K - 1 ) * I + L ): L = K1, K2
END DO
RETURN
```

Subroutine OUTIN

Purpose: to output a matrix of real variables

Other subprograms required: none

This routine is used for the print out of a matrix of input and computed variables like Δx, Δy, k, P, h, etc.

PSEUDO LANGUAGE DESCRIPTION OF OUTIN:

```
ASSIGN ARRAY AREA FOR VAR, ID
WRITE ID
START DO: K1 = 1, I, IW
K2 = MINO ( K1 + IW - 1, I )
START DO: K = 1, J
WRITE VAR (( K - 1 ) * I + L ): L = K1, K2
```

END DO

RETURN

Subroutine POR

Purpose: to compute rock porosity

Other subprograms required: none

The rock porosity in this study is assumed to be a function of pressure only (9):

$$\phi = \phi_i \left[1 + \beta(P - P_i)\right] \qquad (185)$$

$$\text{where } \phi_i = \phi_i (x,y) \qquad (186)$$

PSEUDO LANGUAGE DESCRIPTION OF POR:

SUBROUTINE POR

ASSIGN ARRAY AREA FOR ϕ, ϕ_i, P, P_i,etc.

COMPUTE ϕ USING EQ. (185) FOR EACH ACTIVE CELL

RETURN

Subroutine PREDIH

Purpose: to predict an unknown variable at the new time step

Other subprograms required: none

This routine uses the technique of linear extrapolation to predict the approximate value of an unknown variable at n+1 time level. The algorithm is

given (t_1,y_1), (t_2,y_2)

find y_3 at t_3

$$y_3 = y_1 + (t_3 - t_1) \frac{(y_2 - y_1)}{(t_2 - t_1)} \qquad (187)$$

At the end of each time step, the values P^{n+1} , h^{n+1} are predicted by using this routine.

PSEUDO LANGUAGE DESCRIPTION OF PREDIH:

SUBROUTINE PREDIH

ASSIGN ARRAY AREA FOR y^n , y^{n-1} , etc.

COMPUTE y^{n+1} BY EQ. (187) FOR EACH ACTIVE CELL

RETURN

Subroutine RELAX

Purpose: to perform relaxation process for unknown variables

Other subprograms required: none

The algorithm for relaxation (27) is:

$$y^{k+1} = y^k + \omega(y^{k+1} - y^k) \qquad (188)$$

PSEUDO LANGUAGE DESCRIPTION OF RELAX:

ASSIGN ARRAY AREA FOR y^k , y^{k+1} , etc.

COMPUTE: y^{k+1} BY EQ. (188) FOR EACH ACTIVE CELL

RETURN

Subroutine RELPER

Purpose: to compute water and steam relative permeabilities

Other subprograms required: none

In the two-phase (water-steam) region of a geothermal reservoir, the relative permeabilities of water and steam can be computed by using Corey's equations (9,28):

$$k_{rw} = \frac{(S_w - S_{wi})^4}{(1 - S_{wi})^4} \qquad (189)$$

$$k_{rs} = \left[1 - \frac{(S_w - S_{wi})}{(S_{wm} - S_{wi})} \right]^2 \left[1 - \frac{(S_w - S_{wi})^2}{(S_{wi} - 1)^2} \right] \qquad (190)$$

where $S_{wi} = 0.05$ (191)

and $S_{wm} = 0.95$ (192)

PSEUDO LANGUAGE DESCRIPTION OF RELPER:

SUBROUTINE RELPER

COMPUTE k_{rw}, k_{rs} USING EQS. (189),...,(192)

RETURN

END

Subroutine RESULT

Purpose: to output results

Other subprograms required: OUTIN

This routine prints out time, time step, average fluid pressure P_{av}, average fluid enthalpy h_{av}, average fluid temperature T_{av}, average produced fluid temperature T_{avp}, maximum material balance error r_m, pressure matrix, enthalpy matrix, temperature matrix, and water saturation matrix. P_{av}, h_{av}, T_{av} and T_{avp} are computed using the

volume weighted equations:

$$P_{av} = \frac{\Sigma P_i V_i}{\Sigma V_i} \qquad (193)$$

$$T_{av} = \frac{\Sigma T_i V_i}{\Sigma V_i} \qquad (194)$$

$$h_{av} = \frac{\Sigma h_i V_i}{\Sigma V_i} \qquad (195)$$

$$T_{avp} = \frac{\Sigma T_{pi} V_i}{\Sigma V_{pi}} \qquad (196)$$

PSEUDO LANGUAGE DESCRIPTION OF RESULT:

SUBROUTINE RESULT

ASSIGN ARRAY AREA FOR q_w, q_{wc}, q_s, q_{sc}, q_h, q_{hc}, P_{av}, h_{av}, T_{av}, T_{avp}, etc.

WRITE t, Δt, P_{av}, h_{av}, T_{av}, T_{avp}, r_m

WRITE q_{wi}, q_{wp}, q_{si}, q_{sp}, q_{hi}, q_{hp}

CALL OUTIN: TO OUTPUT P, h, T, S_w

RETURN

Subroutine ROCKH

Purpose: to compute rock enthalpy

Other subprograms required: none

Rock enthalpy is assumed to be a function of temperature (9):

$$h_r = 2.040615\times10^{9} + 8.498886\times10^{6}T + 3.76427\times10^{3}T^2 \qquad (197)$$

PSEUDO LANGUAGE DESCRIPTION OF ROCKH:

ASSIGN ARRAY AREA FOR T, h_r

COMPUTE h_r USING EQ. (197) OFR EACH ACTIVE CELL

RETURN

Subroutine SIP

Purpose: to solve a pentadiagonal matrix system by SIP

Otner subprograms required: none

The odd-even version of SIP is used. The algorithm is given by eqs. (112),...,(131).

PSEUDO LANGUAGE DESCRIPTION OF SIP:

SUBROUTINE SIP

ASSIGN ARRAY AREA FOR a, b, c, d, e, f, U, U1, α, AA, CC, EE, FF, y, etc.

SET AA, CC, EE, FF, y ALL ZERO

COMPUTE d_i EQ. (101)

START DO: I1 = 1, MAX

START DO: I2 = 1, NPAR

RESM = 0

START DO: K = 1, M

i = ACTIVE CELL INDEX

COMPUTE AG, AH, EE, AA, BB, CC, FF, y BY EQS. (112),...,(119)

END DO

COMPUTE U BY EQ. (120)

START DO: K = 1, M

DU1 = U

COMPUTE AG, AH, FF, CC, BB, AA, EE, y BY EQS. (123),...,(130)

END DO

COMPUTE U BY EQ. (131)

TEST FOR CONVERGENCE USING EQ. (109)

IF (CONVERGENCE OK) THEN

U = U + U1

ELSE

END DO

END IF

RETURN

Sub routine TITLE

Purpose: to identify the simulation run

Other subprograms required: none

PSEUDO LANGUAGE DESCRIPTION OF TITLE:

SUBROUTINE TITLE

ASSIGN ARRAY AREA FOR J

READ J

WRITE J

RETURN

Subroutine TRANSM

Purpose: to compute transmissibility terms

Other subprograms required: none

PSEUDO LANGUAGE DESCROPTION OF TRANSM:

SUBROUTINE TRANSM

ASSIGN ARRAY AREA FOR T_{wx}, T_{sx}, T_{hx}, T_{cx}, T_{wy}, T_{sy}, T_{hy}, T_{cy}, T_{hwy}, T_{hsx}, T_{hwy}, T_{hsy}, etc.

START DO: K = 1, M

i = ACTIVE CELL INDEX

IF ($IPHASE_i$ .EQ. 1 .OR. 2) COMPUTE T_{wxi} : EQ. (47)

IF ($IPHASE_i$ .EQ. 3 .OR. 3) COMPUTE T_{sxi} : EQ. (45)

T_{hxi} = EQ. (56)

T_{cxi} = EQ. (58)

IF ($IPHASE_i$ .EQ. 1 .OR. 2) COMPUTE T_{wyi} : EQ. (48)

IF ($IPHASE_i$ .EQ. 3 .OR. 2) COMPUTE T_{syi} : EQ. (46)

T_{hyi} = EQ. (57)

T_{cyi} = EQ. (59)

END DO

RETURN

Subroutine UPSTRM

Purpose: to perform upstream weighting of variables

Other subprograms required: none

This routine is used to ' upstream weigh ' an interblock variable $v_{i-\frac{1}{2}}$ or $v_{i-\frac{1}{2}\eta}$. Consider the following cell configuration:

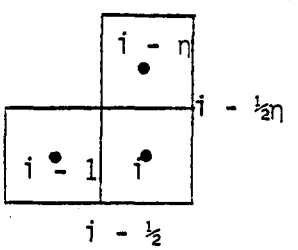

Fig. 6 Interblock cell configuration

If $P_{i-1} > P_i$, then $v_{i-\frac{1}{2}} = v_{i-1}$, otherwise $v_{i-\frac{1}{2}} = v_i$ (198)

If $P_{i-\eta} > P_i$, then $v_{i-\frac{1}{2}\eta} = v_{i-\eta}$, otherwise $v_{i-\frac{1}{2}\eta} = v_i$ (199)

PSEUDO LANGUAGE DESCRIPTION OF UPSTRM:

ASSIGN ARRAY AREA FOR TX, TY, X, Y, Q, etc.

START DO: K = 1, M

i = ACTIVE CELL INDEX

$TX_i = X_i$

IF (Q_{i-1} .GT. Q_i) $TX_i = X_{i-1}$

$TY_i = Y_i$

IF (Q_{i-n} .GT. Q_i) $TY_i = Y_{i-n}$

END DO

RETURN

Subroutine WELL

Purpose: to compute fluid and energy flow rates in wells

Other subprograms required: none

Sources (injection wells) and sinks (production wells) are read in the simulator by positive and negative mass flow rates (q_t) respectively.

For a well in the compressed-water region,

$$q_w = q_t \qquad (200)$$

$$q_s = 0 \qquad (201)$$

$$q_h = q_w h \qquad (202)$$

For a well in the water-steam region (9),

$$\sigma_s = \frac{k_{rs}}{\left(k_{rs} + \frac{\rho_w \mu_s}{\rho_s \mu_w} k_{rw} \right)} \qquad (203)$$

$$q_s = \sigma_s q_t \qquad (204)$$

$$q_w = q_t - q_s \qquad (205)$$

$$q_h = q_s h_s + q_w h_w \qquad (206)$$

For a well in the superheated- steam region,

$$q_w = 0 \qquad (207)$$

$$q_s = q_t \qquad (208)$$

$$q_h = q_s h \qquad (209)$$

PSEUDO LANGUAGE DESCRIPTION OF WELL

SUBROUTINE WELL

ASSIGN ARRAY AREA FOR KWX, KWY, q_t, q_h, q_w, q_s, h_w, h_s, h, etc.

START DO: K = 1, NW

j = WELL INDEX

IF ($IPHASE_j$ .EQ. 1) THEN

COMPUTE q_w, q_s, q_h USING EQS. (200),...,(202)

END IF

IF ($IPHASE_j$ .EQ. 2) THEN

COMPUTE σ_s, q_w, q_s, q_h USING EQS. (203),...,(206)

END IF

IF ($IPHASE_j$ .EQ. 3) THEN

COMPUTE q_w, q_s, q_h USING EQS. (205),...,(209)

```
END IF
END DO
RETURN
```

CHAPTER THREE

RESULTS

3.1 Testing of Simulator: CGS

The geothermal simulator CGS is tested using two different sets of geothermal data. The first is the hypothetical data presented by Mercer and Faust (9). The second is the East Mesa geothermal field data presented by Morris and Campbell (29). A typical computer simulation output is shown in the appendix.

3.2 Simulation Results 1: Mercer and Faust Problem

In this test of the simulator CGS, the hypothetical data (9) of which the initial pressure and temperature are approximately equal to those in the Wairakei field of New Zealand are used. The reservoir, a compressed-water (hydrothermal) type, is taken to be homogeneous in properties. The centimeter-gram-second (CGS) units are used. The reservoir grid with the six production wells, the original field data (9) and the program run parameters are shown as follows.

A 16 x 11 reservoir grid is used to overlay the reservoir:

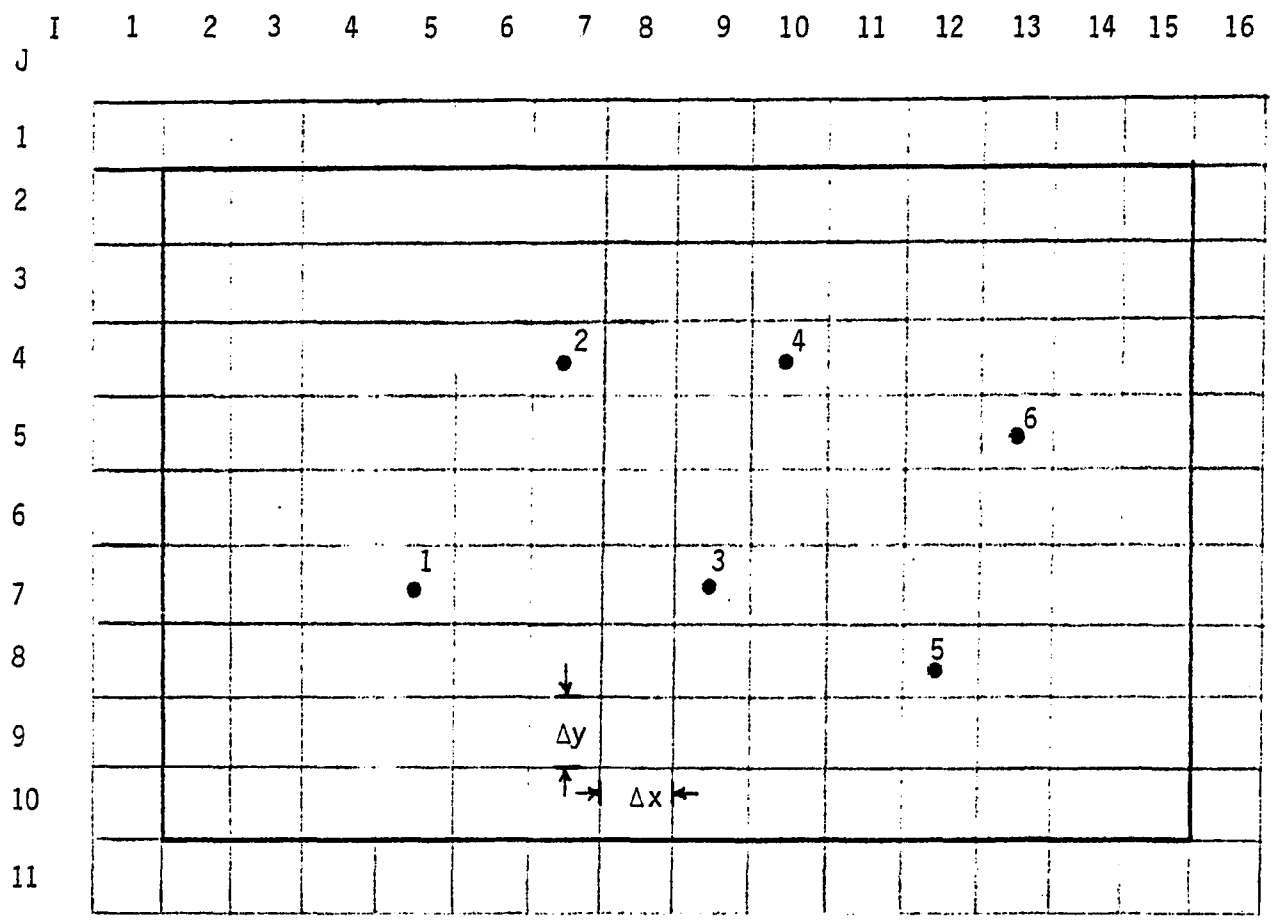

Fig. 7 Reservoir grid for Mercer and Faust problem

2	Well number
●	Production well
———	Reservoir boundary
Δx	3.9286×10^4 cm
Δy	3.8889×10^4 cm

Parameter	Value
k	2.5×10^{-11} cm^2
K_m	3.2×10^{5} ergs/sec-cm-^{o}C
ϕ	0.1
ρ_r	2.5 g/cm^3
β	7.25×10^{-11} cm^2/dyne
Δz	5.0×10^{4} cm
x	5.5×10^{5} cm
y	3.5×10^{5} cm
P_i	6.895×10^{7} dynes/cm^2
h_i	1.047×10^{10} ergs/g
ρ_i	0.8148 g/cm^3
T_i	242.1 ^{o}C
q_1	-2.0×10^{4} g/sec
q_2	-1.5×10^{4} g/sec
q_3	-1.25×10^{4} g/sec
q_4	-1.75×10^{4} g/sec
q_5	-2.0×10^{4} g/sec
q_6	-1.5×10^{4} g/sec

Table 1 Data given in Mercer and Faust (9)

In addition to the above data, the following are used in this test of the simulator CGS.

Parameter	Value
h_{ri}	4.3188×10^9 ergs/g
S_{wi}	1.0
S_{si}	0.0
ω_p	0.6
ω_h	1.0
ε_m	0.01
ε	0.001
Δt	2.592×10^6 sec
t_s	3.1104×10^7 sec

Table 2 Program run parameters

For the purpose of comparing results with those of Mercer and Faust (9), the same time step Δt used by these authors in their simulation is used. Thus the simulator is run for 3.1104×10^7 sec (360 days) using a fully implicit 2.592×10^6 sec (30-day) time step.

The simulation results of average fluid pressure P_{av}, average fluid enthalpy h_{av}, average fluid temperature T_{av}, average produced fluid temperature T_{avp} and maximum absolute relative mass balance error r_m are summarized in the following table.

n	t	P_{av}	h_{av}	T_{av}	T_{avp}	r_m
time step	sec $\times 10^7$	dynes/cm^2 $\times 10^8$	ergs/g $\times 10^{11}$	^oC $\times 10^3$	^oC $\times 10^3$	fraction $\times 10^{-4}$
1	0.259200*	0.675643	0.104702	0.242222	0.242327	0.325168
2	0.518400	0.658165	0.104702	0.242246	0.242384	0.290940
3	0.777600	0.641146	0.104702	0.242270	0.242422	0.263557
4	1.036800	0.624134	0.104702	0.242293	0.242454	0.236175
5	1.296000	0.607115	0.104702	0.242317	0.242483	0.198524
6	1.555200	0.590088	0.104702	0.242341	0.242511	0.164295
7	1.814400	0.573058	0.104703	0.242365	0.242538	0.130067
8	2.073600	0.556026	0.104703	0.242388	0.242565	0.095839
9	2.332800	0.538990	0.104703	0.242413	0.242591	0.075302
10	2.592000	0.521947	0.104703	0.242436	0.242617	0.030805
11	2.851200**	0.505383	0.104703	0.242445	0.242336	0.044497
12	3.110400	0.489443	0.104704	0.242445	0.241884	0.078725

Table 3 Simulation results of Mercer and Faust problem

$\Delta t = 0.259200 \times 10^7$ sec (30 days)

* The geothermal system remains as compressed-water phase from time step 1 to 10.

** Wells nos. 4 and 5 are two-phase wells at time steps 11 and 12.

Simulation results indicate that the whole reservoir remains as compressed-water phase from time 0 sec to 2.592000×10^7 sec (300 days). At time 2.851200×10^7 sec (330 days), well nos. 4 and 5 are two-phase type producing both water and steam. This change of phase after the 300-day period is also reported in Mercer and Faust (9).

From table 3, it can be seen that the average fluid pressure drops to P_{av} are almost isothermal and isoenthalpic. As expected, there are only very small increases in the average fluid temperature T_{av} and the average fluid enthalpy h_{av}. Also, the average produced fluid temperature increases very little in each time step from 0 sec to 2.592×10^7 sec (300 days). Nominally, it should remain the same throughout this period. However, it starts to drop after this 300-day period, at this time the reservoir has become two-phase in two of its sinks as mentioned above. In the 300-day simulation period, the maximum material balance error is decreasing in each time step and is in the order of 10^{-4} in time steps 1 to 7, in the order of 10^{-5} in time steps 8 to 10. The following table compares the results obtained in this simulation with those reported in Mercer and Faust (9) in the 300-day simulation period:

Content	Mercer and Faust	CGS results
model	finite element type 96 nodes and 77 elements	finite difference type 16 x 11 grid 176 cells
matrix method	Gauss-Doolittle	SIP
time step Δt	fully implicit 30-day	fully implicit 30-day
fraction mass produced	0.08	0.0033
energy produced	2.74×10^{22} ergs	2.71×10^{22} ergs
phase changes	after 10 time steps	after 10 time steps
P_{av} drops	Yes	Yes
T_{av} changes	isothermal	isothermal
h_{av} changes	small	very small
average material balance error	0.0116 %	0.00181 %

Table 4 Comparisions between CGS results and those of Mercer and Faust (9)

As can be seen from the above table, the comparisions are with acceptable limits.

The table below shows the number of iterations per time step for solving the pressure eq. (80) and that for the enthalpy eq. (88).

time step	no. of iterations pressure eq. (75)	no. of iterations enthalpy eq. (83)
1	7	1
2	8	1
3	8	1
4	8	1
5	8	1
6	8	1
7	8	1
8	8	1
9	8	1
10	8	1
11	7	1
12	8	1

Table 5 Number of iterations per time step

(Convergence criterion $\varepsilon = 0.001$)

The average execution computer time using CGS for simulating the Mercer and Faust problem for a 360-day period is 27.65 IBM 370/158 CPU seconds. Thus for the 16 x 11 reservoir grid and 12 time steps used for this simulation, the average CPU time is 0.013 seconds per grid block-time step. From table 5, there are 106 iterations. This corresponds to an average CPU time of 0.00012 seconds per grid block-time step-iteration. Coats (30) reported a figure of 0.016 CDC6600 CPU seconds per grid block-time step for simulating a two-dimensional single-well geothermal problem with a grid size of 10 x 5. This 0.016 figure is considered to be a better figure as compared to an approximate value of 0.01 seconds per grid block-time step in the author's semi-implicit models (30). Again, the CDC6600 computer is a faster machine than the IBM 370/158. Thus the index of 0.013 seconds per grid block-time step obtained by using the simulator CGS in the run can be considered to be a very efficient figure.

To gain more insight into the speed of simulation of CGS, the above simulation problem is run using the same data as before except in this run the time step Δt is set equal to 1.55520×10^7 sec (180 days), six times as large as the previous time step. The results are summarized in the following table.

n	t	P_{av}	h_{av}	T_{av}	T_{avp}	r_m
time step	sec $\times 10^7$	dynes/cm^2 $\times 10^8$	ergs/g $\times 10^{11}$	^oC $\times 10^3$	^oC $\times 10^3$	fraction $\times 10^{-4}$
1	1.555200	0.590225	0.104702	0.242340	0.242495	0.068457
2	3.110400	0.488982	0.104702	0.242429	0.241619	0.058188

Table 6 Simulation results of Mercer and Faust problem

$\Delta t = 1.555200 \times 10^7$ sec (180 days)

The results obtained in this run are very close to those obtained before (see table 3). Actually, this run gives even lower average material balance error, which is 0.00063 % for the two time steps. The reason for this lower value is unclear; it is probably due to less machine roundoff errors involved in this run in which two time steps are used instead of 12 time steps as used in the last run. The results of this run indicate that the simulator CGS can be a very stable one, that is, large time steps in the order of hundreds of days may be used, leading to efficient simulation of geothermal systems for a long production period, say 30 years.

3.3 Simulation Results 2: East Mesa Field Problem

In this test of the simulator CGS, the heterogeneous reservoir data of the East Mesa field (a hydrothermal type) of the Imperial Valley of California are used (29). These data were prepared for the simulation of the production behavior of the East Mesa field by

using a three-dimensional, two-phase simulator developed by Intercomp Resource Development and Engineering, Inc.of Houston, Texas (30). Thus, the current test is to utilize and modify part of the original three-dimensional data to fit the two-dimensional capability of CGS. In particular, the conceptual East Mesa field model (29) with a peripheral fluid injection pattern as the main feature is selected for the current simulation test. As the original data are in conventional oil field units, these units will be used in this test as CGS is provided with routines that can convert those units into the centimeter-gram-second computational units used by CGS. Also, the output will be in conventional oil units to be uniform with the input data.

A 12 x 17 grid is used to overlay this reservoir model. In this model, there are nine injection wells and thirteen production wells. The permeability and porosity values are taken to be uniform for each column of cells (29). The following diagram depicts the above information:

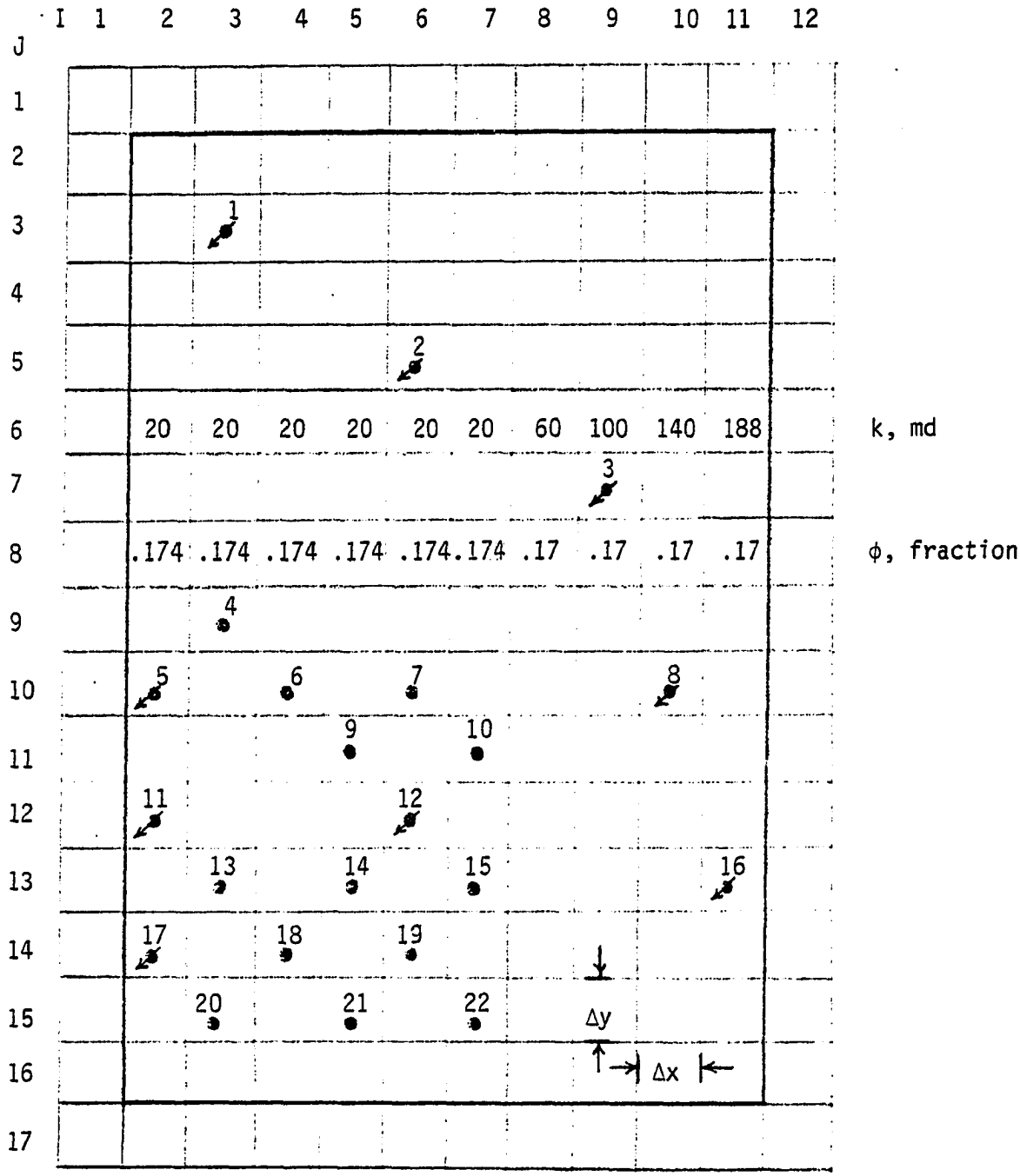

Fig. 8 Reservoir grid for East Mesa field problem

4 Well number
● Production well
1 Well number
Injection well
Reservoir boundary
Δx 1056 ft
Δy 1056 ft

The following data are used in this simulation test:

Parameter	Value
ρ_i	56.594 lb/cu. ft
ρ_{wi}	56.594 lb/cu. ft
ρ_r	156 lb/cu. ft
h_{ri}	153.131 BTU/lb
S_{wi}	1.0
S_{si}	0.0
β	4.0×10^{-6} psi^{-1}
K_m	35.0 BTU/(day-ft-^oF)
Δz	1500 ft
x	10560 ft
y	15840 ft
P_i	2100 psia
h_i	302.952 BTU/lb
T_i	330.1 ^oF
total production	2.21×10^8 lb/day
each sink produces	0.17×10^8 lb/day
total injection	2.16×10^8 lb/day
each source injects	0.24×10^8 lb/day
injection fluid temperature	200 ^oF
ω_p	0.6
ω_h	1.0
ε_m	0.01
ε	0.001
Δt	120 days
t_s	600 days

Table 7 Data for East Mesa field problem

The simulation results of average fluid pressure P_{av}, average fluid enthalpy h_{av}, average fluid temperature T_{av}, average produced fluid temperature T_{avp} and maximum absolute relative mass balance error r_m are summarized in the following table.

n	t	P_{av}	h_{av}	T_{av}	T_{avp}	r_m
time step	days $\times 10^3$	psia $\times 10^4$	BT /lb $\times 10^3$	^oF $\times 10^3$	^oF $\times 10^3$	fraction $\times 10^{-4}$
1	0.120000	0.207295	0.302944	0.330144	0.330987	0.295479
2	0.240000	0.205063	0.302945	0.330182	0.331201	0.064861
3	0.360000	0.202913	0.302945	0.330219	0.331292	0.204193
4	0.480000	0.200781	0.302946	0.330256	0.331346	0.533304
5	0.600000	0.198651	0.302950	0.330293	0.331389	0.838392

Table 8 Simulation results of East Mesa field problem

Simulation results indicate that the whole reservoir remains as compressed-water phase from time 0 to 600 days. During this simulation period, the pressure drops are quite small. This is due to the injection of fluid into the reservoir, which helps maintain the reservoir pressure. In this run, the total injection rate (2.16×10^8 lb/day) is approximately equal to the total production rate (2.21×10^8 lb/day). Thus the reservoir system should be declining (if any) at a very low rate. In this simulation, the pressure drops are usually isoenthalpic and isothermal. Also, the average produced

fluid temperature increases very little in each time step from 0 day to 600 days. This is due to the decrease in well pressure at constant enthalpy, resulting in very slight increase in temperature, as can be seen in the pressure-enthalpy diagram for water (fig. 1). In this simulation period of 600 days, the material balance error is in the order of 10^{-4} and the average value is 0.387246×10^{-4}.

3.4 Conclusions

Based on this study, the following conclusions can be drawn:

1. A mathematical model using two nonlinear coupled partial differential equations with pressure P and enthalpy h as two unknown variables can be used to describe the transport of heat and fluid flow in geothermal systems.
2. A finite difference model based on the P-h model can be used to simulate the multi-phase fluid and heat flow in geothermal systems.
3. A two-dimensional, two-phase computer simulator CGS using the sequential numerical method to solve the pressure and the enthalpy equations is made.
4. A very competitive index of 0.013 computer CPU seconds per grid block-time step performed by CGS is reported.
5. The efficiency of CGS is due to the use of sequential method to solve two simultaneous equations; this method can reduce the amount of computational work by a factor of four as opposed to that by using conventional simultaneous solution technique in reservoir simulation.

6. The use of SIP as the matrix solution method is adequate for solving geothermal finite difference equations; it gives fast, accurate and stable results in this study.

7. The average material balance error given by CGS is of the order of 10^{-4} in this study, indicating that CGS can be a very stable computer simulator.

8. The simulation results of the Mercer and Faust problem using CGS compare favorably with those of the original authors(9), showing CGS is a valid simulator.

9. Both simulations of the Mercer and Faust problem and the East Mesa field problem indicate that for geothermal systems remaining in compressed-water phase, the pressure drops will be under isothermal and isoenthalpic conditions.

10. The simulation results of the East Mesa field problem show that reservoir pressure maintenance can be done by injecting fluid into the geothermal field.

11. The current simulator CGS can be used to determine the optimum injection and production rates and/or the well spacing pattern such that the maximum amount of heat can be extracted from the geothermal reservoir for the purpose of generating electricity in a given period of time.

12. The current simulator CGS can be used, with modifications, to study geothermal fluid flow in fractured systems and/or saline systems.

Nomenclature

A coefficient matrix or multiplying constant

A' modified matrix of A

A_i, B_i, C_i, E_i, F_i coefficients of L and U matrices

A_x, A_y cross-sectional area to x-, y- direction flow

AX, AY x-, y- transmissibility

a, b, c, e, f coefficients of pentadiagonal matrix

a_{hi}, b_{hi}, c_{hi}, e_{hi}, f_{hi} coefficients of enthalpy equation

a_{pi}, b_{pi}, c_{pi}, e_{pi}, f_{pi} coefficients of pressure equation

B adding constant or water influx constant

b reservoir thickness

C_{vr} specific heat at constant volume of reservoir rock and contained fluids

D right hand side vector of matrix equations

d_i, d_{hi}, d_{pi} right hand side coefficients of matrix equation, enthalpy equation and pressure equation

E energy or internal energy

g_i, h_i SIP factorization coefficients

H $h/10^7$

h geothermal fluid enthalpy

h_r, h_s, h_w rock, steam and water enthalpy

I number of cells in x- direction

i unit vector or cell index in x- direction

J number of cells in y- direction

j unit vector or cell index in y- direction

K_m thermal conductivity

k absolute permeability

k_{rs}, k_{rw} steam, water relative permeability

L lower triangular matrix or length of reservoir

M mass

m medium

MIP mass in place

N number of cells in grid

P geothermal fluid pressure

p $P/10^7$

Q net heat conducted to reservoir

q mass flow rate per unit volume of reservoir

q_h energy flow rate per unit volume of reservoir

R residual vector

r relative error

S saturation

s number of SIP iteration parameters in a cycle

T geothermal fluid temperature or transmissibility term

t time

U internal energy or upper triangular matrix

V grid block volume

v variable or intermediate variable to be solved in SIP

v_{fi} initial specific volume of saturated liquid

v_{gi} initial specific volume of saturated steam

$\bar{v}$ phase average velocity

v' modified variable of v

W width of reservoir or total mass

X unknown vector

x Cartesian coordinate or steam quality or unknown variable

y Cartesian coordinate or unknown variable

Greek alphabets

α iteration parameter

β rock compressibility

δ change in x in SIP

Δt time increment, $t^{n+1} - t^n$

Δx x-increment

Δy y-increment

ε error tolerance

η maximum number of cells in the x-direction of grid

$\bar{\lambda}$ heat flow associated with conduction and dispersion

μ geothermal fluid viscosity

π constant pi

ρ geothermal fluid density

σ flow coefficient of steam in two-phase region

ϕ rock porosity

ω relaxation parameter

Subscripts and Superscripts

av average

c capillary or cumulative or current

D dimensionless

e influx fluid

H, h heat or enthalpy

i cell index or initial

j phase index

k iteration counter

L loss

max maximum

n time level or any time period

P, p pressure or produced

r relative or rock or SIP iteration parameter index

s simulation or steam

t total

w water

References

1. Toronyi, R. M. and Farouq Ali, S. M.: "Two-Phase, Two-Dimensional Simulation of a Geothermal Reservoir," Soc. Pet. Eng. J. (June, 1977) 171-183.
2. Faust, C. R. and Mercer, J. W.: "Mathematical Modeling of Geothermal Systems," paper presented at the Second United Nations Symposium on the Development and Use of Geothermal Resources, San Francisco, May 20-29, 1975.
3. Whiting, R. L. and Ramey, H. J., Jr.: "Application of Material and Energy Balances to Geothermal Steam Production," J. Pet. Tech. (July, 1969) 893-900.
4. Harlow, F. H. and Pracht, W. E.: "A Theoretical Study of Geothermal Energy Extraction," J. Geophys. Research (1972) 77, No. 35, 7038-7048.
5. Gould, T. L.: "Vertical Two-Phase Steam-Water Flow in Geothermal Wells," J. Pet. Tech. (August, 1974) 833-842.
6. Garg, S. K., Pritchett, J. W., and Brownell, D. H., Jr.: "Transport of Mass and Energy in Porous Media," paper presented at the Second United Nations Symposium on the Development and Use of Geothermal Resources, San Francisco, May 20-29, 1975.
7. Lasseter, T. J., Witherspoon, P. A., and Lippmann, M. J.: "Multiphase Multidimensional Simulation of Geothermal Reservoirs," paper presented at the Second United Nations Symposium on the Development and Use of Geothermal Resources, San Francisco, May 20-29, 1975.

8. Robinson, R. J. and Morse, R. A.: "A Study of the Effects of Various Reservoir Parameters on the Performance of Geothermal Reservoirs," paper presented at the Second United Nations Symposium on the Development and Use of Geothermal Resources, San Francisco, May 20-29, 1975.

9. Mercer, J. W. and Faust, C. R.: "Simulation of Water- and Vapor-Dominated Hydrothermal Reservoirs," paper SPE 5520 presented at the SPE-AIME 50th Annual Fall Meeting, Dallas, Sept. 28-Oct. 1, 1975.

10. Tansev, E., Startzman, R. A. and Cooper, A. M.: "Predicting Pressure Loss and Heat Transfer in Geothermal Wellbores," paper SPE 5584 presented at the SPE-AIME 50th Annual Fall Meeting, Dallas, Sept. 28-Oct. 1, 1975.

11. Toronyi, R. M. and Farouq Ali, S. M.: "Two-Phase, Two-Dimensional Simulation of a Geothermal Reservoir and the Wellbore System," paper SPE 5521 presented at the SPE-AIME 50th Annual Fall Meeting, Dallas, Sept. 28-Oct. 1, 1975.

12. Martin, J. C.: "Analysis of Internal Steam Drive in Geothermal Reservoirs," J. Pet. Tech. (Dec., 1975) 1493-1499.

13. Faust, C. R. and Mercer, J. W.: "An Analysis of Finite-Difference and Finite-Element Techniques for Geothermal Reservoir Simulation," paper SPE 5742 presented at the SPE-AIME Fourth Symposium on Numerical Simulation of Reservoir Performance, Los Angeles, Feb. 19-20, 1976.

14. Brigham, W. E., and Morrow, W. B.: "p/Z Behavior for Geothermal Steam Reservoirs," Soc. Pet. Eng. J. (Dec., 1977) 407-412.

15. Thomas, L. K. and Pierson, R. G.: "Three-Dimensional Geothermal Reservoir Simulation," Soc. Pet. Eng. J. (April, 1978) 151-161.

16. White, D. E., Muffler, L. P. J., and Truesdell, A. H.: "Vapor-Dominated Hydrothermal Systems Compared with Hot-Water Systems," Economic Geol. (1971) 66, 75-97.

17. Crichlow, H. B.: Modern Reservoir Engineering -- A Simulation Approach, Prentice-Hall, Inc., N. J. (1977).

18. Peaceman, D. W.: Fundamentals of Numerical Reservoir Simulation, Elsevier Scientific Publishing Co., Amsterdam (1977).

19. Douglas, J., Jr., Peaceman, D. W., and Rachford, H. H.,Jr.: "A Method for Calculating Multi-Dimensional Immiscible Displacement," Trans. AIME (1959) 216, 297-306.

20. Stone, H. L.: "Iterative Solutions of Implicit Approximations of Multidimensional Partial Differential Equations," SIAM J. Numerical Analysis (1968) 5, 530-558.

21. Weinstein, H. G., Stone, H. L. and Kwan, T. V.: "Simultaneous Solution of Multiphase Reservoir Flow Equations," Soc. Pet. Eng. J. (June, 1970) 99-110.

22. Suarez, A. and Farouq Ali, S. M.: "A Comparative Evaluation of Different Versions of the Strongly Implicit Procedure (SIP)," paper SPE 5732 presented at the SPE-AIME Symposium on Numerical Simulation of Reservoir Performance, Los Angeles, Feb. 19-20, 1976.

23. Al-Marhoun, M. A.: "Optimal Numerical Procedure to Solve Two-Dimensional Three-Phase Petroleum Reservoir Simulator," Ph. D. Dissertation, University of Oklahoma, Norman, Oklahoma (1978).

24. Marateck, S. L.: Fortran, Academic Press, Inc., N. Y. (1977).

25. Ross, W. F.: "1974 Lake Arrow Workshop," Computer (1975) 8, 6, 21.

26. Irvine, T. F., Jr. and Hartnett, J. P.: Steam and Air Tables in SI Units, Hemisphere Publishing Corp., Washington, D. C., (1976).

27. Hornbeck, R. W.: Numerical Methods, Quantum Publishers, Inc., N. Y. (1975).

28. Corey, A. T.: "The Interrelation Between Gas and Oil Relative Permeabilities," Producers Monthly (1954) 19, 38-41.

29. Morris, C. W. and Campbell, D. A.: "A Three-Dimensional Simulation Study of the East Mesa Field," paper SPE 8229 presented at the SPE-AIME 54th Fall Annual Technical Conference and Exhibition, Las Vegas, Sept. 23-26, 1979.

30. Coats, K. H.: "Geothermal Reservoir Modelling," paper SPE 6892 presented at the SPE-AIME 52nd Annual Fall Technical Conference and Exhibition, Denver, Oct. 9-12, 1977.

Appendix

A Sample of CGS Output

SIMULATION RESULTS 2
TIME = 0.240000E+03 DAYS
TIME STEP = 0.120000E+03 DAYS
AVERAGE FLUID PRESSURE = 0.205063E+04 PSIA
AVERAGE FLUID ENTHALPY = 0.302945E+03 BTU/LB
AVERAGE FLUID TEMPERATURE = 0.330182E+03 DEGREES FAHRENHEIT
AVERAGE PRODUCED FLUID TEMPERATURE = 0.331201E+03 DEGREES FAHRENHEIT
MAXIMUM ABSOLUTE RELATIVE MASS BALANCE ERROR = 0.648613E-05

WELL TABLES
WELL TYPE 1 FOR INJECTION WELL 2 FOR PRODUCTION WELL

WELL NO.	I	J	LOCATION	WELL TYPE	WATER FLOW RATE, LB/DAY	CUMULATIVE, LB
1	3	3		1	0.240000E+08	0.575999E+10
2	6	5		1	0.240000E+08	0.575999E+10
3	9	7		1	0.240000E+08	0.575999E+10
4	3	9		2	-0.170000E+08	-0.407999E+10
5	2	10		1	0.240000E+08	0.575999E+10
6	4	10		2	-0.170000E+08	-0.407999E+10
7	6	10		2	-0.170000E+08	-0.407999E+10
8	10	10		1	0.240000E+08	0.575999E+10
9	5	11		2	-0.170000E+08	-0.407999E+10
10	7	11		2	-0.170000E+08	-0.407999E+10
11	2	12		1	0.240000E+08	0.575999E+10
12	6	12		1	0.240000E+08	0.575999E+10
13	3	13		2	-0.170000E+08	-0.407999E+10
14	5	13		2	-0.170000E+08	-0.407999E+10
15	7	13		2	-0.170000E+08	-0.407999E+10

16	11	13	1	0.240000E+08	0.575999E+1
17	2	14	1	0.240000E+08	0.575999E+1
18	4	14	2	-0.170000E+08	-0.407999E+1
19	6	14	2	-0.170000E+08	-0.407999E+1
20	3	15	2	-0.170000E+08	-0.407999E+1
21	5	15	2	-0.170000E+08	-0.407999E+1
22	7	15	2	-0.170000E+08	-0.407999E+1

TOTAL WATER INJECTION = 0.518398E+11 LB
TOTAL WATER PRODUCTION = 0.530397E+11 LB

WELL NO.	I	J	LOCATION	WELL TYPE	STEAM FLOW RATE, LB/DAY	CUMULATIVE, LB
1	3	3		1	0.0	0.0
2	6	5		1	0.0	0.0
3	9	7		1	0.0	0.0
4	3	9		2	0.0	0.0
5	2	10		1	0.0	0.0
6	4	10		2	0.0	0.0
7	6	10		2	0.0	0.0
8	10	10		1	0.0	0.0
9	5	11		2	0.0	0.0
10	7	11		2	0.0	0.0
11	2	12		1	0.0	0.0
12	6	12		1	0.0	0.0
13	3	13		2	0.0	0.0
14	5	13		2	0.0	0.0

15	7	13	2	0.0	0.0
16	11	13	1	0.0	0.0
17	2	14	1	0.0	0.0
18	4	14	2	0.0	0.0
19	6	14	2	0.0	0.0
20	3	15	2	0.0	0.0
21	5	15	2	0.0	0.0
22	7	15	2	0.0	0.0

TOTAL STEAM INJECTION = 0.0 LB
TOTAL STEAM PRODUCTION = 0.0 LB

WELL NO.	I	J	LOCATION	WELL TYPE	HEAT FLOW RATE, BTU/DAY	CUMULATIVE, BTU
1	3	3		1	0.403452E+10	0.968285E+12
2	6	5		1	0.403452E+10	0.968285E+12
3	9	7		1	0.403452E+10	0.968285E+12
4	3	9		2	-0.515011E+10	-0.123603E+13
5	2	10		1	0.403452E+10	0.968285E+12
6	4	10		2	-0.515011E+10	-0.123603E+13
7	6	10		2	-0.515011E+10	-0.123603E+13
8	10	10		1	0.403452E+10	0.968285E+12
9	5	11		2	-0.515011E+10	-0.123603E+13
10	7	11		2	-0.515011E+10	-0.123603E+13
11	2	12		1	0.403452E+10	0.968285E+12
12	6	12		1	0.403452E+10	0.968285E+12

13	3	13	2	-0.515011E+10	-0.123603E+13
14	5	13	2	-0.515010E+10	-0.123603E+13
15	7	13	2	-0.515011E+10	-0.123603E+13
16	11	13	1	0.403452E+10	0.968285E+12
17	2	14	1	0.403452E+10	0.968285E+12
18	4	14	2	-0.515010E+10	-0.123603E+13
19	6	14	2	-0.515011E+10	-0.123603E+13
20	3	15	2	-0.515011E+10	-0.123603E+13
21	5	15	2	-0.515010E+10	-0.123603E+13
22	7	15	2	-0.515011E+10	-0.123603E+13

TOTAL HEAT INJECTION = 0.871455E+13 BTU
TOTAL HEAT PRODUCTION = 0.160683E+14 BTU

PRESSURE, PSIA

I	1	2	3	4	5	6
J						
1	0.0	0.0	0.0	0.0	0.0	0.0
2	0.0	0.27849E+04	0.27960E+04	0.26946E+04	0.25944E+04	0.25043E+04
3	0.0	0.27806E+04	0.29150E+04	0.26994E+04	0.25897E+04	0.25096E+04
4	0.0	0.26483E+04	0.26666E+04	0.26040E+04	0.25603E+04	0.25338E+04
5	0.0	0.25033E+04	0.25044E+04	0.24948E+04	0.25182E+04	0.26491E+04
6	0.0	0.23615E+04	0.23571E+04	0.23564E+04	0.23722E+04	0.23998E+04
7	0.0	0.22273E+04	0.22088E+04	0.22044E+04	0.22169E+04	0.22392E+04
8	0.0	0.21130E+04	0.20477E+04	0.20369E+04	0.20529E+04	0.20890E+04
9	0.0	0.20640E+04	0.18320E+04	0.18422E+04	0.18688E+04	0.19131E+04
10	0.0	0.22455E+04	0.18851E+04	0.16293E+04	0.16654E+04	0.16593E+04
11	0.0	0.20612E+04	0.18307E+04	0.16338E+04	0.15011E+04	0.16761E+04
12	0.0	0.21034E+04	0.17385E+04	0.15696E+04	0.15373E+04	0.18027E+04
13	0.0	0.17816E+04	0.14447E+04	0.13631E+04	0.12705E+04	0.14835E+04
14	0.0	0.17900E+04	0.14011E+04	0.11606E+04	0.12040E+04	0.12678E+04
15	0.0	0.14560E+04	0.12009E+04	0.11788E+04	0.11098E+04	0.13139E+04
16	0.0	0.13682E+04	0.12712E+04	0.12353E+04	0.12469E+04	0.13875E+04
17	0.0	0.0	0.0	0.0	0.0	0.0

I	7	8	9	10	11	12
J						
1	0.0	0.0	0.0	0.0	0.0	0.0
2	0.24131E+04	0.23533E+04	0.23318E+04	0.23210E+04	0.23165E+04	0.0
3	0.24147E+04	0.23511E+04	0.23287E+04	0.23175E+04	0.23128E+04	0.0
4	0.24197E+04	0.23460E+04	0.23222E+04	0.23103E+04	0.23053E+04	0.0
5	0.24242E+04	0.23344E+04	0.23120E+04	0.22993E+04	0.22935E+04	0.0
6	0.23409E+04	0.23065E+04	0.23000E+04	0.22843E+04	0.22771E+04	0.0
7	0.22521E+04	0.22698E+04	0.23019E+04	0.22647E+04	0.22545E+04	0.0
8	0.21507E+04	0.22022E+04	0.22264E+04	0.22259E+04	0.22233E+04	0.0
9	0.20338E+04	0.21300E+04	0.21698E+04	0.21896E+04	0.21898E+04	0.0
10	0.18925E+04	0.20560E+04	0.21200E+04	0.21693E+04	0.21565E+04	0.0
11	0.17377E+04	0.19833E+04	0.20604E+04	0.21012E+04	0.21122E+04	0.0

12	0.17858E+04	0.19366E+04	0.20107E+04	0.20545E+04	0.20770E+04	0.0
13	0.15876E+04	0.18718E+04	0.19649E+04	0.20182E+04	0.20608E+04	0.0
14	0.15759E+04	0.18318E+04	0.19264E+04	0.19771E+04	0.20037E+04	0.0
15	0.14840E+04	0.18006E+04	0.18990E+04	0.19475E+04	0.19691E+04	0.0
16	0.15947E+04	0.18034E+04	0.18882E+04	0.19330E+04	0.19526E+04	0.0
17	0.0	0.0	0.0	0.0	0.0	0.0

ENTHALPY, BTU/LB

I	1	2	3	4	5	6
J						
1	0.0	0.0	0.0	0.0	0.0	0.0
2	0.0	0.30295E+03	0.30295E+03	0.30295E+03	0.30295E+03	0.30295E+03
3	0.0	0.30295E+03	0.30295E+03	0.30295E+03	0.30295E+03	0.30295E+03
4	0.0	0.30295E+03	0.30295E+03	0.30295E+03	0.30295E+03	0.30295E+03
5	0.0	0.30295E+03	0.30295E+03	0.30295E+03	0.30295E+03	0.30295E+03
6	0.0	0.30295E+03	0.30295E+03	0.30295E+03	0.30295E+03	0.30295E+03
7	0.0	0.30295E+03	0.30295E+03	0.30295E+03	0.30295E+03	0.30295E+03
8	0.0	0.30295E+03	0.30295E+03	0.30295E+03	0.30295E+03	0.30295E+03
9	0.0	0.30295E+03	0.30295E+03	0.30295E+03	0.30295E+03	0.30295E+03
10	0.0	0.30295E+03	0.30295E+03	0.30295E+03	0.30295E+03	0.30295E+03
11	0.0	0.30295E+03	0.30295E+03	0.30295E+03	0.30295E+03	0.30295E+03
12	0.0	0.30295E+03	0.30295E+03	0.30295E+03	0.30295E+03	0.30295E+03
13	0.0	0.30295E+03	0.30295E+03	0.30295E+03	0.30295E+03	0.30295E+03
14	0.0	0.30295E+03	0.30295E+03	0.30295E+03	0.30295E+03	0.30295E+03
15	0.0	0.30295E+03	0.30295E+03	0.30295E+03	0.30295E+03	0.30295E+03
16	0.0	0.30295E+03	0.30295E+03	0.30295E+03	0.30295E+03	0.30295E+03
17	0.0	0.0	0.0	0.0	0.0	0.0

I	7	8	9	10	11	12
J						
1	0.0	0.0	0.0	0.0	0.0	0.0
2	0.30295E+03	0.30295E+03	0.30295E+03	0.30295E+03	0.30295E+03	0.0
3	0.30295E+03	0.30295E+03	0.30295E+03	0.30295E+03	0.30295E+03	0.0
4	0.30295E+03	0.30295E+03	0.30295E+03	0.30295E+03	0.30295E+03	0.0
5	0.30295E+03	0.30295E+03	0.30295E+03	0.30295E+03	0.30295E+03	0.0
6	0.30295E+03	0.30295E+03	0.30295E+03	0.30295E+03	0.30295E+03	0.0
7	0.30295E+03	0.30295E+03	0.30295E+03	0.30295E+03	0.30295E+03	0.0
8	0.30295E+03	0.30295E+03	0.30295E+03	0.30295E+03	0.30295E+03	0.0
9	0.30295E+03	0.30295E+03	0.30295E+03	0.30295E+03	0.30295E+03	0.0
10	0.30295E+03	0.30295E+03	0.30295E+03	0.30295E+03	0.30295E+03	0.0
11	0.30295E+03	0.30295E+03	0.30295E+03	0.30295E+03	0.30295E+03	0.0
12	0.30295E+03	0.30295E+03	0.30295E+03	0.30295E+03	0.30295E+03	0.0
13	0.30295E+03	0.30295E+03	0.30295E+03	0.30295E+03	0.30295E+03	0.0
14	0.30295E+03	0.30295E+03	0.30295E+03	0.30295E+03	0.30295E+03	0.0
15	0.30295E+03	0.30295E+03	0.30295E+03	0.30295E+03	0.30295E+03	0.0
16	0.30295E+03	0.30295E+03	0.30295E+03	0.30295E+03	0.30295E+03	0.0
17	0.0	0.0	0.0	0.0	0.0	0.0

TEMPERATURE, DEGREES FAHRENHEIT

I	1	2	3	4	5	6
J						
1	0.0	0.0	0.0	0.0	0.0	0.0
2	0.0	0.32893E+03	0.32891E+03	0.32908E+03	0.32925E+03	0.32941E+03
3	0.0	0.32894E+03	0.32871E+03	0.32907E+03	0.32926E+03	0.32940E+03
4	0.0	0.32916E+03	0.32913E+03	0.32924E+03	0.32931E+03	0.32936E+03
5	0.0	0.32941E+03	0.32941E+03	0.32942E+03	0.32938E+03	0.32916E+03
6	0.0	0.32965E+03	0.32966E+03	0.32966E+03	0.32963E+03	0.32959E+03
7	0.0	0.32988E+03	0.32991E+03	0.32992E+03	0.32990E+03	0.32986E+03
8	0.0	0.33007E+03	0.33019E+03	0.33020E+03	0.33018E+03	0.33012E+03
9	0.0	0.33016E+03	0.33055E+03	0.33054E+03	0.33049E+03	0.33042E+03
10	0.0	0.32985E+03	0.33046E+03	0.33090E+03	0.33084E+03	0.33085E+03
11	0.0	0.33016E+03	0.33056E+03	0.33089E+03	0.33112E+03	0.33082E+03
12	0.0	0.33009E+03	0.33071E+03	0.33100E+03	0.33106E+03	0.33060E+03
13	0.0	0.33064E+03	0.33121E+03	0.33135E+03	0.33151E+03	0.33115E+03
14	0.0	0.33063E+03	0.33129E+03	0.33170E+03	0.33162E+03	0.33152E+03
15	0.0	0.33120E+03	0.33163E+03	0.33167E+03	0.33179E+03	0.33144E+03
16	0.0	0.33134E+03	0.33151E+03	0.33157E+03	0.33155E+03	0.33131E+03
17	0.0	0.0	0.0	0.0	0.0	0.0

I	7	8	9	10	11	12
J						
1	0.0	0.0	0.0	0.0	0.0	0.0

2	0.32956E+03	0.32966E+03	0.32970E+03	0.32972E+03	0.32973E+03	0.0
3	0.32956E+03	0.32967E+03	0.32971E+03	0.32973E+03	0.32973E+03	0.0
4	0.32955E+03	0.32968E+03	0.32972E+03	0.32974E+03	0.32975E+03	0.0
5	0.32954E+03	0.32970E+03	0.32974E+03	0.32976E+03	0.32977E+03	0.0
6	0.32969E+03	0.32974E+03	0.32976E+03	0.32978E+03	0.32979E+03	0.0
7	0.32984E+03	0.32981E+03	0.32975E+03	0.32982E+03	0.32983E+03	0.0
8	0.33001E+03	0.32992E+03	0.32988E+03	0.32988E+03	0.32989E+03	.0
9	0.33021E+03	0.33005E+03	0.32998E+03	0.32994E+03	0.32994E+03	0.0
10	0.33045E+03	0.33017E+03	0.33006E+03	0.32998E+03	0.33000E+03	0.0
11	0.33071E+03	0.33030E+03	0.33016E+03	0.33010E+03	0.33008E+03	0.0
12	0.33063E+03	0.33038E+03	0.33025E+03	0.33017E+03	0.33014E+03	0.0
13	0.33097E+03	0.33049E+03	0.33033E+03	0.33024E+03	0.33016E+03	.0
14	0.33099E+03	0.33055E+03	0.33039E+03	0.33031E+03	0.33026E+03	0.0
15	0.33115E+03	0.33061E+03	0.33044E+03	0.33036E+03	0.33032E+03	0.0
16	0.33096E+03	0.33060E+03	0.33046E+03	0.33038E+03	0.33035E+03	0.0
17	0.0	0.0	0.0	0.0	0.0	0.0

WATER SATURATION

J \ I	1	2	3	4	5	6
1	0.0	0.0	0.0	0.0	0.0	0.0
2	0.0	0.10000E+01	0.10000E+01	0.10000E+01	0.10000E+01	0.10000E+01
3	0.0	0.10000E+01	0.10000E+01	0.10000E+01	0.10000E+01	0.10000E+01
4	0.0	0.10000E+01	0.10000E+01	0.10000E+01	0.10000E+01	0.10000E+01
5	0.0	0.10000E+01	0.10000E+01	0.10000E+01	0.10000E+01	0.10000E+01
6	0.0	0.10000E+01	0.10000E+01	0.10000E+01	0.10000E+01	0.10000E+01
7	0.0	0.10000E+01	0.10000E+01	0.10000E+01	0.10000E+01	0.10000E+01
8	0.0	0.10000E+01	0.10000E+01	0.10000E+01	0.10000E+01	0.10000E+01
9	0.0	0.10000E+01	0.10000E+01	0.10000E+01	0.10000E+01	0.10000E+01
10	0.0	0.10000E+01	0.10000E+01	0.10000E+01	0.10000E+01	0.10000E+01
11	0.0	0.10000E+01	0.10000E+01	0.10000E+01	0.10000E+01	0.10000E+01
12	0.0	0.10000E+01	0.10000E+01	0.10000E+01	0.10000E+01	0.10000E+01
13	0.0	0.10000E+01	0.10000E+01	0.10000E+01	0.10000E+01	0.10000E+01
14	0.0	0.10000E+01	0.10000E+01	0.10000E+01	0.10000E+01	0.10000E+01
15	0.0	0.10000E+01	0.10000E+01	0.10000E+01	0.10000E+01	0.10000E+01
16	0.0	0.10000E+01	0.10000E+01	0.10000E+01	0.10000E+01	0.10000E+01
17	0.0	0.0	0.0	0.0	0.0	0.0

J \ I	7	8	9	10	11	12
1	0.0	0.0	0.0	0.0	0.0	0.0
2	0.10000E+01	0.10000E+01	0.10000E+01	0.10000E+01	0.10000E+01	0.0
3	0.10000E+01	0.10000E+01	0.10000E+01	0.10000E+01	0.10000E+01	0.0
4	0.10000E+01	0.10000E+01	0.10000E+01	0.10000E+01	0.10000E+01	0.0
5	0.10000E+01	0.10000E+01	0.10000E+01	0.10000E+01	0.10000E+01	0.0
6	0.10000E+01	0.10000E+01	0.10000E+01	0.10000E+01	0.10000E+01	0.0
7	0.10000E+01	0.10000E+01	0.10000E+01	0.10000E+01	0.10000E+01	0.0
8	0.10000E+01	0.10000E+01	0.10000E+01	0.10000E+01	0.10000E+01	0.0
9	0.10000E+01	0.10000E+01	0.10000E+01	0.10000E+01	0.10000E+01	0.0
10	0.10000E+01	0.10000E+01	0.10000E+01	0.10000E+01	0.10000E+01	0.0
11	0.10000E+01	0.10000E+01	0.10000E+01	0.10000E+01	0.10000E+01	0.0
12	0.10000E+01	0.10000E+01	0.10000E+01	0.10000E+01	0.10000E+01	0.0
13	0.10000E+01	0.10000E+01	0.10000E+01	0.10000E+01	0.10000E+01	0.0
14	0.10000E+01	0.10000E+01	0.10000E+01	0.10000E+01	0.10000E+01	0.0
15	0.10000E+01	0.10000E+01	0.10000E+01	0.10000E+01	0.10000E+01	0.0
16	0.10000E+01	0.10000E+01	0.10000E+01	0.10000E+01	0.10000E+01	0.0
17	0.0	0.0	0.0	0.0	0.0	0.0